

Flavor Phenomenology of Light Dark Vectors

Jordi Folch Eguren^{*a}, Sophie Klingel^b, Emmanuel Stamou^{†a},
Mustafa Tabet^{‡a}, Robert Ziegler^{§b,c}

^a*Department of Physics, TU Dortmund, D-44221 Dortmund, Germany*

^b*Institute for Theoretical Particle Physics, KIT, 76128 Karlsruhe, Germany*

^c*Institute for Theoretical Physics, Heidelberg University, 69120 Heidelberg, Germany*

May 2, 2024

Abstract

Light dark matter with flavor-violating couplings to fermions may be copiously produced in the laboratory as missing energy from decays of SM particles. Here we study the effective Lagrangian of a light dark vector with generic dipole or vector couplings. We calculate the resulting two-body decay rates of mesons, baryons and leptons as a function of the dark vector mass and show that existing experimental limits probe UV scales as large as 10^{12} GeV. We also derive the general RGEs in order to constrain the flavor-universal UV scenario, where all flavor violation arises radiatively proportional to the CKM matrix.

1 Introduction

In recent years light new particles interacting very weakly with the Standard Model (SM) have gained increased interest. The so far negative results on searches for heavy particles above the electroweak scale at the LHC and high-intensity experiments have increased the interest in less explored scenarios, with additional degrees of freedom beyond the SM with masses at sub-GeV scales. Such particles can be motivated by dynamics addressing the Strong CP Problem (in case of the QCD axion) or the origin of neutrino masses (in case of sterile neutrinos), but probably the main motivation is the possibility that such light particles could be connected to the origin of particle dark matter (DM) [1].

In this context a popular scenario is the dark photon [2, 3], which is either itself DM or is the only mediator (“Vector Portal”) between the SM and a hidden “dark sector”, which contains one or several DM particles [4, 5], see Ref. [6] for a review. The term “dark photon” usually refers to a light vector particle coupled to the SM only via kinetic mixing or dipole operators and that is often taken as the

*jordi.eguren@tu-dortmund.de

†emmanuel.stamou@tu-dortmund.de

‡mustafa.tabet@tu-dortmund.de

§robert.ziegler@kit.edu

only new degree of freedom. Instead, the term Z' is typically reserved for the vast model space of theories of gauged $U(1)'$ extensions of the SM, where also a complete Higgs sector for $U(1)'$ breaking is explicitly present, besides additional matter needed for anomaly cancellation, see, e.g., Ref. [7] for a classification. While the Z' vector boson is often taken to be heavy, with a mass much above the electroweak (EW) scale, this particle can also be much lighter. The resulting coupling patterns are often related to the underlying UV symmetries, see, e.g., Refs. [8–11], and can leave imprints in low-energy phenomenology/anomalies in current data, e.g., in $(g-2)_\mu$ [12] or in low-energy QCD [13]. Beyond perturbative models, light vector particles can also be in the spectrum of light resonances of low-energy, dark strongly coupled sectors, see, e.g., Ref. [14]. To encompass all these cases, we employ in the current work the term “light dark vector” (LDV), which is a massive vector boson with mass much below the EW scale, and sufficiently suppressed couplings to SM particles such that it is stable on collider scales. For the purpose of low-energy phenomenology we leave its UV origin unspecified.

While constraints on light particles have been extensively studied in the context of colliders, beam-dump experiments, astrophysics, and cosmology, their phenomenology at precision flavor experiments has so far received less attention (see Ref. [15, 16] for early studies). Even if flavor-violating couplings may be considered more model-dependent than flavor-diagonal couplings, they can provide for an efficient production of light invisible particles from decays of SM leptons, mesons or baryons. Interestingly, direct searches at laboratory experiments for such two-body decays with missing energy have the potential to probe enormously large scales, as the relevant Lagrangian interactions can be dimension-five, instead of dimension-six as in the case of heavy New Physics. For example, in models with sufficiently light invisible bosons like the QCD axion, precision flavor experiments are sensitive to scales as large as 10^{12} GeV from $K \rightarrow \pi + \text{invis.}$ searches at NA62 [17], 10^{10} GeV from $\mu \rightarrow e + \text{invis.}$ searches at MEG-II [18, 19], Mu3e [20], Mu2e or COMET [21], and 10^8 GeV for $b \rightarrow d/s$ transitions at Belle II [22].¹

The aim of the current work is to systematically study the flavor phenomenology of light dark vector particles (LDVs), both in the quark and the lepton sectors. We restrict the discussion to invisible particles, since after all the main (only) motivation for these particles is the observed DM abundance, and we have in mind scenarios where either the LDV is itself stable on cosmological scales or promptly decays to stable DM particles. This analysis includes scenarios where the LDVs are just sufficiently long-lived to appear as missing energy. This is particularly justified for vector particles lighter than the electron, as their decay into two photons is forbidden by the Landau–Yang theorem [26, 27]. As we shall discuss, the resulting limits on flavor-violating interactions can be as strong as in the axion case, which is not unexpected due to the Goldstone-boson equivalence theorem. In light of past and ongoing experimental searches, it is thus important to systematically study the phenomenological differences between light dark scalars and vectors originating from their distinct helicity and coupling structure.

Earlier works have focused on the case of flavor-violating dipole couplings of a massless dark photon in $\mu \rightarrow e$ and $s \rightarrow d$ transitions [6, 28–32], or considered general interactions and masses, but using only the available experimental limits on three-body decays to neutrinos to study limits from $s \rightarrow d$ and $b \rightarrow s$ transitions [16]. Here instead we consider the case of a light vector particle with generic mass and either dipole or minimal couplings to SM fermions. We work within the framework of a general effective-field-theory (EFT) approach and consider all possible quark flavor-violating transitions except those involving the top quark (where constraints are very weak), and all possible lepton flavor-violating (LFV) transitions. We also discuss the decays of polarized leptons, which play an important role in separating signal from SM background. We derive bounds in the general parameter

¹For the flavor phenomenology of the QCD axion and light invisible axion-like particles see Refs. [16, 18, 22–25].

plane of light-vector mass and the appropriate flavor-changing coupling by comparing theoretical predictions for the decay rates to the experimental bounds from various flavor factories, such as NA62 [33, 34], BaBar [35, 36], CLEO [37], Belle II [38, 39], BES III [40], and TWIST [41]. Whenever not available (as in the case of, e.g., $B \rightarrow K/K^*/\pi + \text{invis.}$ or $D \rightarrow \pi + \text{invis.}$ decays), we derive model-independent limits on the two-body decay rate as a function of the invisible particle mass by recasting experimental data on the three-body decay with two invisible neutrinos. Finally, we also discuss the scenario where the light vector has only flavor-universal couplings to SM fermions in the UV, so that all quark flavor-changing effects in the IR are induced radiatively by the Cabibbo–Kobayashi–Maskawa (CKM) matrix, satisfying the paradigm of Minimal Flavor-Violation (MFV) [42, 43]. For this analysis we derive the relevant renormalization-group equations (RGEs) for both dipole and minimal couplings, and use our results to convert limits on the flavor-changing interactions into limits on flavor-diagonal couplings.

This work is organized as follows. In Section 2 we define our basic setup by providing the effective Lagrangian for dipole and minimal (vector) interactions of the LDV. The resulting phenomenology is studied in the subsequent sections, separately for the quark (Section 3) and lepton (Section 4) sectors, where we present our main results, the model-independent bounds on generic flavor-violating LDV couplings as a functions of its mass. In Section 5 we use these constraints to derive bounds on flavor-universal UV couplings with either dipole or vector interactions from RG-induced flavor violation. We conclude in Section 6. Many technical details are deferred to appendices: Appendix C contains the details and results of our recast of two-body flavor-violating decays with missing energy for generic masses of the invisible particles (extending the analysis for a massless invisible particle in Ref. [22]). Appendix D contains the bounds on flavor-violating couplings in the chiral L/R basis (as opposed to the V/A basis in Section 3 and 4). The complete set of RGEs relevant for Section 5 is given in Appendix B, and Appendix E contains the full expressions of two-body decay rates of mesons, baryons, and polarized leptons, for a generic mass for the light vector. We have also collected the hadronic matrix elements entering the numerical analysis in Appendix E.1. Finally, Appendix A contains a discussion of the EFT description of flavor-violating vector couplings and their possible UV origin.

2 Setup

We extend the SM by a new, neutral, massive vector boson V'_μ with a small mass $m_{V'}$, which arises either by spontaneous symmetry breaking of, e.g., a $U(1)'$ gauge symmetry or by the Stueckelberg mechanism [44–46]. Here we focus on the case where this mass is much below the electroweak scale, and the light dark vector (LDV) is either stable on collider scales or decays into stable invisible particles.

The most general interactions of the LDV with the SM fermions can be parametrized using an EFT approach, by considering the most general operators that respect the unbroken part of the SM gauge group, $SU(3)_c \times U(1)_{\text{em}}$. Here we focus on flavor-violating interactions written without loss of generality in the fermion-mass basis. We can further assume that a possible kinetic mixing between the photon and the LDV, i.e., $\propto \epsilon A^\mu V'_\mu$, has been diagonalized such that V'_μ is also in the mass-eigenstate basis. This diagonalization can be performed equally well for a massless V'_μ (cf. Ref. [29]), and the difference with respect to the massive case is merely that for massless vectors there remains an unphysical ambiguity in the choice of “mass-eigenstate” basis, due to the presence of an unbroken $SO(2)$ symmetry of the free Lagrangian. Thus our setup applies equally well to the “massless dark photon” considered in Ref. [29] in the limit of $m_{V'} \rightarrow 0$.

Below the EW scale the lowest dimensional interactions of the LDV are described by two classes of operators: dipole and vector interactions. Firstly, we consider flavor-violating, dimension-five dipole

interactions of the form

$$\mathcal{L}_D = -\frac{1}{4}V'_{\mu\nu}V'^{\mu\nu} + \frac{m_{V'}^2}{2}V'_\mu V'^\mu + \frac{1}{\Lambda}V'_{\mu\nu}\bar{f}_i\sigma^{\mu\nu}(\mathbb{C}_{ij}^D + i\mathbb{C}_{ij}^{D5}\gamma_5)f_j, \quad (2.1)$$

where $V'_{\mu\nu} = \partial_\mu V'_\nu - \partial_\nu V'_\mu$ is the LDV field strength, $\sigma^{\mu\nu} = \frac{i}{2}[\gamma^\mu, \gamma^\nu]$, and $i \neq j$ denote SM quark or lepton flavors. Λ is the UV-completion scale of the associated dipole couplings \mathbb{C}_{ij}^D and \mathbb{C}_{ij}^{D5} , which are hermitian matrices in flavor space, $(\mathbb{C}_{ij}^D)^* = \mathbb{C}_{ji}^D$ and $(\mathbb{C}_{ij}^{D5})^* = \mathbb{C}_{ji}^{D5}$.

Secondly, we consider flavor-violating couplings of the LDV to SM vector and axial-vector currents. Naively these are dimension-four interactions below the EW scale. However, such flavor-violating couplings violate $U(1)'$ gauge invariance (flavor-violating currents are not conserved), and thus must be proportional to some power of the $U(1)'$ -breaking order parameter, which we take as the vacuum expectation value (VEV) in the dark sector. Therefore, the flavor-violating vector couplings are actually dimension-five or higher, depending on the underlying UV model. In perturbative UV completions the lowest possible scaling is proportional to a single power of the dark VEV, which upon including the dark gauge coupling becomes the LDV mass $m_{V'}$. Normalizing by some UV scale Λ , the flavor-violating vector interactions are

$$\mathcal{L}_V = -\frac{1}{4}V'_{\mu\nu}V'^{\mu\nu} + \frac{m_{V'}^2}{2}V'_\mu V'^\mu + \frac{m_{V'}}{\Lambda}V'_\mu\bar{f}_i\gamma^\mu(\mathbb{C}_{ij}^V + \mathbb{C}_{ij}^{V5}\gamma_5)f_j, \quad (2.2)$$

where again $i \neq j$ denote SM quark or lepton flavors and the vector couplings \mathbb{C}_{ij}^V and \mathbb{C}_{ij}^{V5} are hermitian matrices in flavor space, $(\mathbb{C}_{ij}^V)^* = \mathbb{C}_{ji}^V$ and $(\mathbb{C}_{ij}^{V5})^* = \mathbb{C}_{ji}^{V5}$.

By choosing a scaling that is linear in $m_{V'}/\Lambda$, we ensure that the growth of amplitudes with longitudinally polarized LDVs in initial and/or final states $\propto E/m_{V'}$ as $m_{V'} \rightarrow 0$ is cancelled by the $m_{V'}$ dependence in the interaction. This leads to finite amplitudes in the $m_{V'} \rightarrow 0$ limit (see Refs. [16, 47–50] for related discussions), which are just the amplitudes with the corresponding Goldstone bosons as initial/final states. An explicit example for a UV model that provides this linear scaling is provided by Froggatt–Nielsen type models [51], discussed in Appendix A. However, the linear scaling with $m_{V'}$ is only one possibility. For example, in UV models in which SM fermions do not carry $U(1)'$ charges the scaling can be quadratic in the dark VEV, as the coefficients involve additional powers of the $U(1)'$ breaking scale v' , $\propto m_{V'}v'/\Lambda^2$. An explicit realization of this scenario is also discussed in Appendix A.

The interactions in Eq. (2.1) and (2.2) can also be written in the chiral basis, which is more suited to match explicit UV models. In this basis

$$\begin{aligned} \mathcal{L}_D &= \frac{1}{\Lambda}V'_{\mu\nu}\bar{f}_i\sigma^{\mu\nu}(\mathbb{C}_{ij}^{DL}P_L + \mathbb{C}_{ij}^{DR}P_R)f_j, \\ \mathcal{L}_V &= \frac{m_{V'}}{\Lambda}V'_\mu\bar{f}_i\gamma^\mu(\mathbb{C}_{ij}^{VL}P_L + \mathbb{C}_{ij}^{VR}P_R)f_j, \end{aligned} \quad (2.3)$$

where $\mathbb{C}_{ij}^{DL} = (\mathbb{C}_{ji}^{DR})^*$, $\mathbb{C}_{ij}^{VL} = (\mathbb{C}_{ji}^{VR})^*$, $\mathbb{C}_{ij}^{VR} = (\mathbb{C}_{ji}^{VR})^*$ and the relations between the “V/A” and the “L/R” bases are

$$\mathbb{C}_{ij}^D = \frac{1}{2}(\mathbb{C}_{ij}^{DL} + \mathbb{C}_{ij}^{DR}) = \frac{1}{2}((\mathbb{C}_{ji}^{DR})^* + \mathbb{C}_{ij}^{DR}), \quad \mathbb{C}_{ij}^V = \frac{1}{2}(\mathbb{C}_{ij}^{VL} + \mathbb{C}_{ij}^{VR}), \quad (2.4)$$

$$\mathbb{C}_{ij}^{D5} = \frac{i}{2}(\mathbb{C}_{ij}^{DL} - \mathbb{C}_{ij}^{DR}) = \frac{i}{2}((\mathbb{C}_{ji}^{DR})^* - \mathbb{C}_{ij}^{DR}), \quad \mathbb{C}_{ij}^{V5} = \frac{1}{2}(\mathbb{C}_{ij}^{VR} - \mathbb{C}_{ij}^{VL}). \quad (2.5)$$

Above the EW scale the operators must be expressed in a manifestly $SU(2)_L \times U(1)_Y$ invariant manner. For \mathcal{L}_V this is directly the case after embedding the left- and right-handed fermions in the

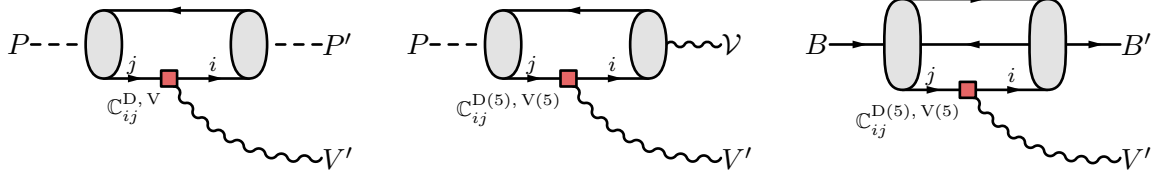


Figure 1: Illustrative Feynman diagrams with a flavor-violating $q_j \rightarrow q_i$ transition in two-body decays of type $P \rightarrow P' + V'$, $P \rightarrow \mathcal{V} + V'$, and $B \rightarrow B' + V'$, in the left, middle, and right panel, respectively.

corresponding $SU(2)_L$ doublets and singlets, respectively. Instead, the dipole operators in \mathcal{L}_D require an additional Higgs insertion, making them dimension-six operators

$$\mathcal{L}_{D6} = \frac{1}{\Lambda_6^2} V'_{\mu\nu} (\bar{F}_i H C_{ij}^D \sigma^{\mu\nu} P_R f_j + \text{h.c.}) , \quad (2.6)$$

with F_i and f_j denoting here $SU(2)_L$ doublets and singlets, respectively, and $H \rightarrow \tilde{H}$, depending on the fermion sector and the hypercharge conventions. The matching to \mathcal{L}_D is provided by identifying $\Lambda_6 = \sqrt{v}\Lambda$, where $v = 174 \text{ GeV}$ is the Higgs VEV.

In the following we derive bounds on the flavor-violating couplings in Eq. (2.1) and (2.2) from hadronic and leptonic decays with missing energy in the final state. This discussion is unaffected by other possible interactions of the LDV with SM fields, in particular flavor-diagonal couplings, as long as these couplings are sufficiently small to ensure that the LDV is invisible on collider scales.

For massive LDVs neither the flavor-violating dipole (Eq. (2.1)) nor the vector (Eq. (2.2)) interactions are UV complete. The UV completion depends on the origin of the mass for the LDV and the corresponding (highly model-dependent) radial mode required for the unitarity of the theory. In turn this implies that unless the complete dark Higgs sector of the theory is specified, there exist perturbative unitarity constraints on the couplings of the LDV, similar to the unitarity constraints from $WW \rightarrow WW$ scattering in the Higgs-less SM. We briefly note that, as long as the flavor bounds are applicable, i.e., LDV masses in the kinematically allowed region, unitarity of $2 \rightarrow 2$ scattering poses constraints on the corresponding couplings that are weaker than those limits by order of magnitudes. We thus refrain from elaborating upon these constraints in the current work. For the case of unitarity bounds on massless fermions with flavor-diagonal couplings coupled to transversely polarized vectors see, e.g., Ref. [52]. The more general case including massive fermions with flavor-violating couplings to LDVs will be presented in Ref. [53].

3 Quark Phenomenology of Light Dark Vectors

In this section we derive bounds on the flavor-violating couplings $C_{ij}^{D(5)}$ in Eq. (2.1) and $C_{ij}^{V(5)}$ in Eq. (2.2) for the quark-flavor transitions: $s \rightarrow d$, $b \rightarrow s$, $b \rightarrow d$, and $c \rightarrow u$. We employ the following three types of two-body decays containing the LDV as an invisible final state²

- $P \rightarrow P' + V'$: pseudoscalar meson to pseudoscalar meson and LDV,
- $P \rightarrow \mathcal{V} + V'$: pseudoscalar meson to vector meson and LDV,

²Three-body decays and neutral meson mixing typically give weaker constraints, e.g., for example LHCb constraints on $B_{(s)} \rightarrow \mu\mu a$ cannot compete with Belle II limits [54].

- $B \rightarrow B' + V'$: baryon to baryon and LDV.

Figure 1 shows representative Feynman diagrams for the three types of decays.

Appendix E contains the analytical expressions for the corresponding decay rates (including the dependence on $m_{V'}$); the relevant form factors are collected in Appendix E.1. Comparing the decay rates to the experimental upper limits on the branching ratios, we set upper bounds on the couplings in the V/A basis³ of Eq. (2.1) and Eq. (2.2), i.e. on the set $\{\mathbb{C}_{ij}^D, \mathbb{C}_{ij}^{D5}, \mathbb{C}_{ij}^V, \mathbb{C}_{ij}^{V5}\}$. The limits are determined as a function of the LDV mass, with range $0 \leq m_{V'}^2 \leq (m_I - m_F)^2 \equiv m_{V',\max}^2$ depending on the masses of the initial, m_I , and final, m_F , states of the decay at hand. Crucially, the form factors depend on the LDV mass and it is, therefore, essential to consider the full form-factor parametrization for an accurate analysis.

The available theoretical and experimental information is summarized in Table 1, where we collect the references for the form factors and relevant experimental limits. Often the experimental collaborations do not provide limits on two-body decays with missing energy. Yet, in some cases there is enough information to extract this bound from available data. We indicate this case by a subindex “ r ” in the last column of the table, and either use existing recasts in the literature or perform our own recast, e.g., to find a bound on $B \rightarrow \pi/K/K^* + \text{invis.}$ from BaBar data on the corresponding three-body decays [35, 36], see Appendix C for details.

Concretely we use our recast for $B \rightarrow K^{(*)} + \text{invis.}$ only for LDV masses above 3 GeV. Note that we can recast only the experimental results of the BaBar collaboration and cannot use the newer Belle measurements, since the Belle collaboration does not provide the event count as a (binned) function of the missing-momentum distribution. We use existing recasts for $B \rightarrow \rho + \text{invis.}$ decays from LEP [55, 56], $B \rightarrow K + \text{invis.}$ decays from Belle II [39, 57] (this recast is limited to masses below $m_{V'} = 3$ GeV), $B \rightarrow K^* + \text{invis.}$ decays from BaBar [36, 57] (below $m_{V'} = 3$ GeV). For invisible baryon decays for which there is no analysis, we derive limits using the total lifetime from the PDG [58] after subtracting all observed channels as in Ref. [22].

For the bound based on $D \rightarrow \pi + \text{invis.}$ decays we use the result of Ref. [22] for $m_{V'} \approx 0$, obtained from recasting CLEO data on $D \rightarrow (\tau \rightarrow \pi\nu)\nu$ [37]. We also perform a recast of these data for LDV masses up to $m_{V'} \approx 0.5$ GeV (which is the upper range of the CLEO data set), assuming the efficiency in all bins to be the same as for $m_{V'} \approx 0$. Note that recasting BES III data [59] on $D \rightarrow \pi\nu\bar{\nu}$ gives weaker constraints [22], although this result does not use the full experimental information. It would be interesting if BES III would provide an explicit two-body recast of their full data set. The collaboration actually does this for the case of two-body hyperon decays $\Lambda_c \rightarrow p + \text{invis.}$, albeit only for “massless” invisible particles. Their signal region in fact covers invisible masses up to 316 MeV, and leads to limits that are much stronger than the ones obtained by saturating the total Λ_c lifetime [22]. As a conservative limit, to be replaced by a dedicated experimental analysis, we multiply their limit for the massless case by a factor 1/2 (since close to the endpoint of the signal region half of the signal events are lost due to energy resolution). We use the resulting bound $\text{BR}(\Lambda_c \rightarrow pV') < 1.6 \times 10^{-4}$ for LDV masses up to 316 MeV, and take lifetime limits above 316 MeV. We notice that a search for the decay $D \rightarrow \pi + X$ would not suffer from two-body SM backgrounds in contrast to hyperon decays, where $\Lambda_c \rightarrow p + \gamma$ contributes to the signal of a massless X , if the photon is missed.

To set constraints on the couplings $\{\mathbb{C}_{ij}^D, \mathbb{C}_{ij}^{D5}, \mathbb{C}_{ij}^V, \mathbb{C}_{ij}^{V5}\}$ we consider dipole (\mathcal{L}_D) and vector interactions (\mathcal{L}_V) separately, and turn on a single coupling at a time. We use the theory predictions in Appendix E together with the form factors in Table 1 (see also Appendix E.1) to calculate the decay rates as a function of the couplings and the LDV mass. The rates are then compared to the experimental limits to obtain the bounds in the mass–coupling plane. We include statistical and systematic uncertainties as

³In Appendix D we show the bounds in the L/R basis.

Quark Transition	Hadronic Process	Form Factors	Experimental Limit
$s \rightarrow d$	$K^+ \rightarrow \pi^+ + V'$	[60, 61]	NA62 [17, 33, 34]
	$\Sigma^+ \rightarrow p + V'$	[32, 62–64]	BES III [65], Lifetime _r [22, 58]
	$\Xi^- \rightarrow \Sigma^- + V'$	[32, 62–64]	Lifetime _r [22, 58]
	$\Xi^0 \rightarrow \Sigma^0 + V'$	[32, 62–64]	Lifetime _r [22, 58]
	$\Xi^0 \rightarrow \Lambda + V'$	[32, 62–64]	Lifetime _r [22, 58]
	$\Lambda \rightarrow n + V'$	[32, 62–64]	Lifetime _r [22, 58]
$b \rightarrow s$	$B^+ \rightarrow K^+ + V'$	[66, 66]	BaBar _r [36], Belle II _r [39, 57]
	$B \rightarrow K^* + V'$	[66, 66]	BaBar _r [36, 57]
	$\Lambda_b \rightarrow \Lambda + V'$	[67, 67]	Lifetime _r [22, 58]
$b \rightarrow d$	$B^+ \rightarrow \pi^+ + V'$	[66, 68]	BaBar _r [35]
	$B \rightarrow \rho + V'$	[66, 66]	LEP _r [55, 56]
	$\Lambda_b \rightarrow n + V'$	[67, 69]	Lifetime _r [22, 58]
$c \rightarrow u$	$D^+ \rightarrow \pi^+ + V'$	[70, 71]	CLEO _r [22, 37]
	$\Lambda_c \rightarrow p + V'$	[72, 72]	BES III [40], Lifetime _r [22, 58]

Table 1: Overview of considered hadron decays with invisibles in the final state. The first column shows the underlying quark-flavor transition, the second the specific hadronic process. The relevant vector and dipole form factors are taken from the references in the third column. The last column contains the references for the experimental upper limits on the respective branching ratios. A subindex “*r*” indicates that a recast of experimental data was needed, see text and Appendix C for details.

follows. For the theory predictions we only use the systematic uncertainties associated with hadronic form factors (these are the most relevant ones), while the treatment of uncertainties of experimental limits depend on their nature: for decays where the experimental collaborations provide two-body interpretations (or a theory recast exists), we add the experimental and form-factor uncertainties in quadrature. In the case where we performed our own two-body recast (as described in Appendix C) we treat theory uncertainties as Gaussian uncertainties smearing the expectation values of the underlying Poisson probability distribution functions.

Our results are summarized in Figures 2 and 3 in which we show the lower bounds on the effective inverse coupling Λ/\mathbb{C}_{ij} for given LDV mass $m_{V'}$. The plots are organized according to the underlying flavor transition, i.e. $s \rightarrow d$, $b \rightarrow s$, $b \rightarrow d$, and $c \rightarrow u$ and we separate dipole $\{\mathbb{C}_{ij}^D, \mathbb{C}_{ij}^{D5}\}$ (Figure 2) and vector couplings $\{\mathbb{C}_{ij}^V, \mathbb{C}_{ij}^{V5}\}$ (Figure 3). Each plot shows the bound on a single coupling for a given quark-flavor transition, with each line corresponding to a particular hadronic decay, excluding the region below. Note that $P \rightarrow P' + V'$ decays are only sensitive to $\{\mathbb{C}_{ij}^D$ and $\mathbb{C}_{ij}^V\}$ couplings, which follows from parity conservation of the strong interactions and the Lorentz structure of the form factors (see Appendix E.1). Also note that dipole operators are dimension-six above the electroweak scale, so in fact the actual UV scale probed is $\Lambda_6 = \sqrt{v\Lambda}$ in all transitions.

3.1 Dark Dipole Interactions

$s \rightarrow d$ Transitions The bounds on the dipole couplings $\{\mathbb{C}_{sd}^D, \mathbb{C}_{sd}^{D5}\}$ are set by $K \rightarrow \pi + \text{invis.}$ and hyperon decays, cf. Table 1 and Figure 2. For the two-body decay $K \rightarrow \pi + \text{invis.}$ we use the bound

provided by the NA62 collaboration [34]. For baryon decays there is an upper limit from BES III [65] on the decay $\Sigma^+ \rightarrow p + \text{invis.}$ with a massless invisible. We estimate the potential reach for this search by extending it to larger invisible masses by assuming that the same experimental limit is valid for the whole kinematic range. This is indicated by a dashed orange line. For all other baryon searches, we set upper limits on branching ratios indirectly as in Ref. [22] by subtracting the measured branching fractions for all relevant hyperon decay channels from unity. Due to this rather weak limit, $K \rightarrow \pi$ sets a much more stringent constraint than hyperon decays, limiting the UV scale $\Lambda/\mathbb{C}_{ij}^D$ to be at least of the order 10^{11} GeV. Note however that the search for $\Sigma^+ \rightarrow p + \text{invis.}$ strenghtens the upper limit by two orders of magnitude compared to the conservative limit estimated with the total lifetime, and thus, out of all baryon decays, it yields the strongest limit of order 10^7 GeV on the scale $\Lambda/\mathbb{C}_{ij}^D$.

Nevertheless baryon decays with missing energy are important for two reasons. The decays to pseudoscalar, such as $K \rightarrow \pi$, are only sensitive to the $\{\mathbb{C}_{ij}^D, \mathbb{C}_{ij}^V\}$ couplings. Thus baryon decays are crucial to constrain the axial coupling $\Lambda/\mathbb{C}_{ij}^{D5}$ (of the order of a few $\times 10^7$ GeV), as there are no two-body decays to vector particles in $s \rightarrow d$ transitions. Moreover, the decay rates of pseudoscalar processes are proportional to the LDV mass for the dipole interaction \mathcal{L}_D (cf. Eq. (E.12)), and thus only baryon decays can constrain \mathbb{C}_{ij}^D for small LDV masses. This can be seen in Figure 2 (upper left panel), where the bounds on \mathbb{C}_{sd}^D from hyperon decays dominate for LDV masses of $m_{V'} \approx 0$ yielding a limit of $\mathcal{O}(10^7 \text{ GeV})$ on the axial coupling $\Lambda/\mathbb{C}_{ij}^{D5}$. This provides a strong motivation for explicit direct searches targeting baryon decays with invisible final states.

$b \rightarrow s$ Transitions The limits on the dipole couplings $\{\mathbb{C}_{bs}^D, \mathbb{C}_{bs}^{D5}\}$ are set by B -meson decays $B \rightarrow K/K^* + \text{invis.}$ and baryon decays $\Lambda_b \rightarrow \Lambda + \text{invis.}$ The limits from the B -meson decays are obtained from our own recast of BaBar data (cf. Appendix C), except for $B^+ \rightarrow K^+ + \text{invis.}$ for LDV masses $m_{V'} < 3 \text{ GeV}$ where we use the recast in Ref. [57] of the recent Belle II measurement of $B^+ \rightarrow K^+ \bar{\nu} \nu$ [39]. We also use the recast in Ref. [57] of the BaBar measurement of $B \rightarrow K^* \bar{\nu} \nu$ [36] below LDV masses of 3 GeV. The limit on unobserved Λ_b decays such as $\Lambda_b \rightarrow \Lambda + \text{invis.}$ is obtained by comparing the SM prediction for the total lifetime with the experimental one inferred from all observed channels, ascribing the difference to the allowed value for the two-body invisible decay [22]. As for $s \rightarrow d$ transitions, decays to pseudoscalar mesons such as $B^+ \rightarrow K^+$ can neither constrain the axial coupling \mathbb{C}_{bs}^{D5} , nor \mathbb{C}_{bs}^D for very small LDV masses. Otherwise, however, they do dominate over the constraint from $\Lambda_b \rightarrow \Lambda$.

In contrast to $s \rightarrow d$ transitions, there is also a decay with vector mesons in the final-state, $B \rightarrow K^*$, which constrains both the \mathbb{C}_{bs}^D and the \mathbb{C}_{bs}^{D5} couplings in the entire LDV mass range, if kinematically allowed. Hence, $B \rightarrow K^*$ decays are complementary to $B \rightarrow K$ decays in constraining $\Lambda/\mathbb{C}_{bs}^D$, setting limits on the UV scale of the order 10^8 GeV, and also dominate the bounds on $\Lambda/\mathbb{C}_{bs}^{D5}$ of similar size, up to a small region where this channel is kinematically closed and $\Lambda_b \rightarrow \Lambda$ decays set the strongest limit, of the order 10^7 GeV. Note that there is an *upper* limit of order 10^8 GeV on $\Lambda/\mathbb{C}_{bs}^D$ at around $m_{V'} \approx 2 \text{ GeV}$ coming from $B \rightarrow K + V'$ decays [57], due to a 2.8σ excess in the latest Belle II measurement of $B^+ \rightarrow K^+ \nu \bar{\nu}$ [39].

$b \rightarrow d$ Transitions The bounds on the dipole couplings $\{\mathbb{C}_{bd}^D, \mathbb{C}_{bd}^{D5}\}$ are obtained from B -meson decays $B \rightarrow \pi/\rho + \text{invis.}$ and baryon decays $\Lambda_b \rightarrow n + \text{invis.}$ The limit on $B \rightarrow \pi$ decays is obtained from our recast of BaBar data (cf. Appendix C), while a limit on $B \rightarrow \rho$ decays from LEP data [55] has been derived in Ref. [56]. Analogously to $b \rightarrow s$ transitions, the pseudoscalar decay $B \rightarrow \pi$ does neither constrain the axial coupling \mathbb{C}_{bd}^{D5} nor \mathbb{C}_{bd}^D for small LDV masses, while the decay to vector mesons $B \rightarrow \rho$ does. Thus the two meson decays are complementary in setting limits on $\Lambda/\mathbb{C}_{bd}^D$, of

the order of 10^8 GeV, while $B \rightarrow \rho$ dominates the bounds on the limits on $\Lambda/\mathbb{C}_{bd}^{\text{D5}}$ of similar size, except for LDV masses above the kinematic threshold where $\Lambda_b \rightarrow n$ decays take over, constraining UV scales up to 10^7 GeV.

$c \rightarrow u$ Transitions Finally, the constraints on the dipole couplings $\{\mathbb{C}_{cu}^{\text{D}}, \mathbb{C}_{cu}^{\text{D5}}\}$ are set by $D \rightarrow \pi + \text{invis.}$ and the baryonic process $\Lambda_c \rightarrow p + \text{invis.}$ For $D \rightarrow \pi$ and LDV masses $m_{V'} \lesssim 0.5$ GeV, we performed a recast of the CLEO data set (analogous to the B -decay recasts in Appendix C). The result is shown as a solid, blue line in the bottom panel of Fig. 2. CLEO has only collected data up to masses of $m_{V'} \approx 0.5$ GeV, but we also show the potential bound that could be obtained above this mass by extrapolating the bound for massless invisible particles [22] to the whole kinematic range, which we indicate by a dashed blue line.

For $\Lambda_c \rightarrow p$ we show two limits in the bottom panel of Fig. 2: solid, orange lines denote the bound obtained from simply saturating the total Λ_c lifetime, i.e., $\text{BR}(\Lambda_c \rightarrow p + V') < 1$, while the green line indicates the 95% CL bound obtained from the BES III [40] result for “massless” invisible particles, $\text{BR}(\Lambda_c \rightarrow p + V) < 8.0 \times 10^{-5}$ at 90% CL, which in fact covers invisible masses up to 316 MeV and are multiplied by a factor 1/2, see the discussion in the beginning of this section. We estimate the potential reach for a search extending to larger invisible masses by assuming that the same experimental limit below 316 MeV is also valid above, and indicate this extrapolation by a dashed, green line. We observe that the strongest limits on $\Lambda/\mathbb{C}_{cu}^{\text{D}}$ are set by the BES III search for a “massless” LDV in $\Lambda_c \rightarrow p$ decays, which are valid for $m_{V'} \lesssim 316$ MeV and are of the order of 10^7 GeV. Between $316 \text{ MeV} \lesssim m_{V'} \lesssim 500 \text{ MeV}$ a limit of similar size is obtained from $D \rightarrow \pi$ decays, recasting CLEO data on $D \rightarrow (\tau \rightarrow \pi\nu)\nu$. The only available limit on LDV masses above 0.5 GeV arises from the total Λ_c lifetime, which sets limits of order 10^5 GeV. Naively extrapolating the limits from CLEO on $D \rightarrow \pi$ and BES III on $\Lambda_c \rightarrow p$ decays to higher LDV masses instead suggests that present bounds could be strengthened by two orders of magnitude, if BES III would either analyze the available searches for $\Lambda_c \rightarrow p$ decays with extended signal regions, or use available data on $D \rightarrow \pi\nu\bar{\nu}$ to set a limit on the two-body decay.

Currently only $\Lambda_c \rightarrow p$ decays are capable to set constraints on the axial coupling $\Lambda/\mathbb{C}_{cu}^{\text{D5}}$, of the order of 10^5 GeV and 10^7 GeV for LDV masses above and below 316 MeV, respectively. Besides extending the search for $\Lambda_c \rightarrow p + V'$ to higher LDV masses, this also motivates dedicated searches for other processes such as $D \rightarrow \rho + \text{invis.}$ or $D_s \rightarrow K^* + \text{invis.}$ at current or future experiments.

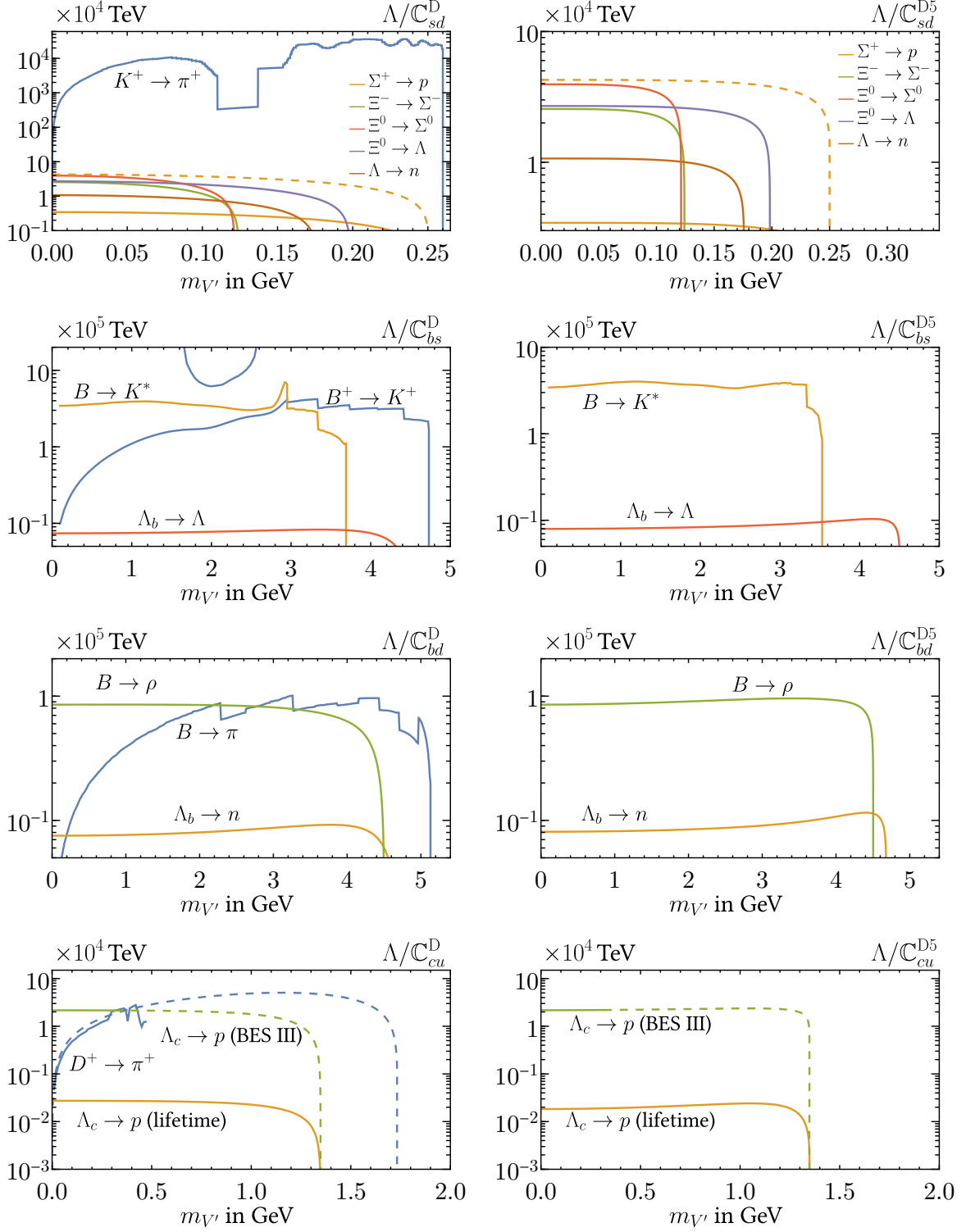


Figure 2: Lower limits on quark-flavor violating dipole couplings $\Lambda/|C_{ij}^D|$ (left column) and $\Lambda/|C_{ij}^{D5}|$ (right column) of the LDV for $s \rightarrow d, b \rightarrow s, b \rightarrow d, c \rightarrow u$ transitions @95% $CL_{(s)}$. See text for details.

3.2 Dark Vector Interactions

$s \rightarrow d$ Transitions The limits on the vector couplings $\{\mathbb{C}_{sd}^V, \mathbb{C}_{sd}^{V5}\}$ are shown in Figure 3. As for dipole couplings, the relevant constraints arise from $K \rightarrow \pi$ and hyperon decays, see Table 1. Analogous to the dipole case, the limit from BES III on the decay $\Sigma^+ \rightarrow p + \text{invis.}$ for a massless invisible is tentatively assumed to be valid for the whole kinematic range. The limit on the scale is indicated by a dashed orange line. $K \rightarrow \pi$ decays dominate the limits on $\Lambda/\mathbb{C}_{sd}^V$, restricting UV scales up to 10^{12} GeV, but cannot constrain the axial coupling $\Lambda/\mathbb{C}_{sd}^{V5}$, where hyperon decays set the only available bounds of the order of 10^7 GeV. All limits are non-vanishing when the LDV mass is taken to zero, which is due to the choice of the prefactor in \mathcal{L}_V linear in the LDV mass, see Eq. (2.2). This corresponds to the gauge-less limit where the longitudinal polarization of the LDV is essentially a Goldstone boson. With this scaling the flavor-violating decay is similar to the SM decay $t \rightarrow Wb$, which also remains finite in the gauge-less $g \rightarrow 0$ limit, since the top quark dominantly decays to the charged Goldstone Higgs, which couples only via Yukawas to the quarks. Different choices for the prefactor, corresponding to specific UV completions, would result in bounds that would vanish in the limit of massless LDVs, with a LDV mass dependence that can be obtained by rescaling the limits presented here.

$b \rightarrow s$ Transitions The constraints on the vector couplings $\mathbb{C}_{bs}^V, \mathbb{C}_{bs}^{V5}$ are obtained from B -meson decays $B \rightarrow K/K^* + \text{invis.}$ and the baryonic decays $\Lambda_b \rightarrow \Lambda + \text{invis.}$ $B^+ \rightarrow K^+$ sets the strongest constraint on $\Lambda/\mathbb{C}_{bs}^V$ of the order of 10^8 GeV, but cannot constrain the axial coupling $\Lambda/\mathbb{C}_{bs}^{V5}$. Here the dominant constraints are set by $B \rightarrow K^*$ decays, also of the order of 10^8 GeV, apart from the region where this channel is kinematically closed and $\Lambda_b \rightarrow \Lambda$ takes over and sets limits on the UV scales up to 10^6 GeV. Again there is an *upper* limit of order 10^{12} GeV on $\Lambda/\mathbb{C}_{bs}^V$ at around $m_{V'} \approx 2$ GeV coming from $B \rightarrow K + V'$ decays [57], due to a 2.8σ excess from the latest Belle II measurement of $B^+ \rightarrow K^+ \nu \bar{\nu}$ [39].

$b \rightarrow d$ Transitions The bounds on the vector couplings $\mathbb{C}_{bd}^V, \mathbb{C}_{bd}^{V5}$ arise from B -meson decays $B \rightarrow \pi/\rho + \text{invis.}$ and the baryonic decays $\Lambda_b \rightarrow n + \text{invis.}$ Analogously to $b \rightarrow s$ transitions $B \rightarrow \pi$ decay sets the strongest constraint on $\Lambda/\mathbb{C}_{bd}^V$ of the order of 10^8 GeV, while $\Lambda/\mathbb{C}_{bd}^{V5}$ is limited to about the same values by $B \rightarrow \rho$ decays, up to LDV masses at the kinematic threshold where $\Lambda_b \rightarrow n$ decays dominate the bound of order 10^6 GeV.

$c \rightarrow u$ Transitions Finally, the bounds on the vector couplings $\mathbb{C}_{cu}^V, \mathbb{C}_{cu}^{V5}$ are set by the decays $D \rightarrow \pi + \text{invis.}$ and $\Lambda_c \rightarrow p + \text{invis.}$ Meson decays $D \rightarrow \pi$ dominate the bound on $\Lambda/\mathbb{C}_{cu}^V$ of order 10^8 GeV, while only baryon decays $\Lambda_c \rightarrow p$ can constrain the axial coupling $\Lambda/\mathbb{C}_{cu}^{V5}$ at order 10^5 and 10^7 GeV, using the total lifetime and the extrapolation of the BES III measurement, respectively, analogous to the dipole case. Again, it would be interesting if BES III could extend their search for $\Lambda_c \rightarrow p + V'$ to higher invisible masses, as this is expected to strengthen the present bound on the UV scale by two orders of magnitude.

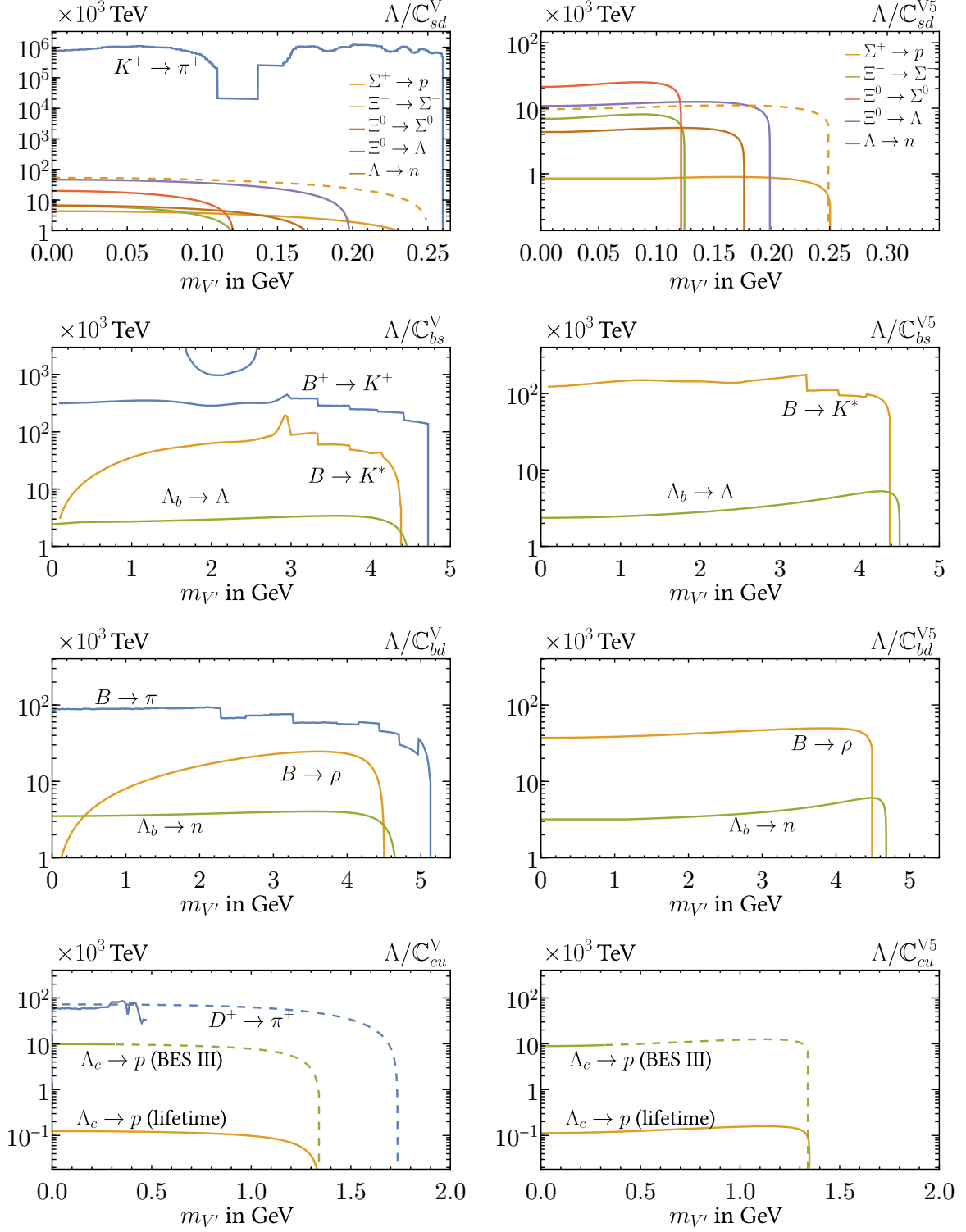


Figure 3: Lower limits on quark-flavor violating vector couplings $\Lambda/|C_{ij}^V|$ (left column) and $\Lambda/|C_{ij}^{V5}|$ (right column) of the LDV for $s \rightarrow d, b \rightarrow s, b \rightarrow d, c \rightarrow u$ transitions @95% $CL(s)$. See text for details.

LFV Transition	Experimental Limit
$\mu \rightarrow e$	TWIST [41], Jodidio _r [18, 73]
$\tau \rightarrow e$	Belle II [38]
$\tau \rightarrow \mu$	Belle II [38]

Table 2: The LFV transitions relevant for the two-body decays $\ell \rightarrow \ell' + V'$ and the corresponding relevant experimental measurements. The subindex “*r*” indicates that a recast of experimental data was needed.

4 Lepton Phenomenology of Light Dark Vectors

In this section we present the bounds on the flavor-violating couplings in Eq. (2.1) and (2.2) from LFV decays $\ell \rightarrow \ell' + V'$ for lepton-flavor transitions $\mu \rightarrow e$, $\tau \rightarrow e$, and $\tau \rightarrow \mu$. There are three main differences to the quark-sector analysis: *i*) there is no hadronic input required, *ii*) the total decay rates only depend on the combination $|\mathbb{C}_{ij}^D|^2 + |\mathbb{C}_{ij}^{D5}|^2$ and $|\mathbb{C}_{ij}^V|^2 + |\mathbb{C}_{ij}^{V5}|^2$, and *iii*) for the case of $\mu \rightarrow e$ transitions one can profit from polarization in order to suppress SM background from Michel decays. This allows us to distinguish between \mathbb{C}_{ij}^V and \mathbb{C}_{ij}^{V5} using the angular distribution of the outgoing electron.

Concretely, for $\mu \rightarrow e$ we restrict the discussion to three benchmark scenarios, depending on the angular dependence of the differential two-body LFV decay rate in the limit of $m_e = m_{V'} = 0$

$$\frac{d\Gamma(\mu \rightarrow e + V')}{d\cos\theta} \propto (1 + A \cos\theta), \quad (4.1)$$

where θ is the angle between the outgoing electron momentum and the muon polarization. We distinguish three benchmark cases: isotropic decays ($A = 0$), “ $V - A$ ” structure $A = -1$, and “ $V + A$ ” structure $A = +1$. Clearly polarization does not help to distinguish an LFV signal from the SM background for the SM case $A = -1$. Thus one can only rely on the monochromatic electron as the signal, which leads to weaker bounds than in the other cases $A = 0, +1$ [18]. Interestingly, many proposals have been put forward to look for this decay at present and future high-luminosity muon facilities [18–21], which are sensitive also to invisible LDVs. We take present constraints on LFV transitions from the references indicated in Table 2, and compare them to the predictions for (polarized) lepton decay rates calculated in Appendix E.5.

$\mu \rightarrow e$ Transitions The bounds from $\mu \rightarrow e + \text{invis.}$ decays on dipole and vector couplings are shown in Fig. 4. We derive them employing constraints from experiments conducted at TRIUMF, both by the TWIST collaboration [41] in 2015 (left panel) and Jodidio et al. [73] in 1986 (right panel). For the latter, we use the recast of Ref. [18]. The three curves in Fig. 4 show the bounds for the three benchmark scenarios for chiral structures, corresponding to $\mathbb{C}_{e\mu}^D = 0$ or $\mathbb{C}_{e\mu}^{D5} = 0$ for $A = 0$, and $\mathbb{C}_{e\mu}^D = \pm i\mathbb{C}_{e\mu}^{D5}$ for $A \approx \pm 1$ in the upper panel, while in the lower panel they correspond to $\mathbb{C}_{e\mu}^V = 0$ or $\mathbb{C}_{e\mu}^{V5} = 0$ for $A = 0$, and $\mathbb{C}_{e\mu}^V = \pm\mathbb{C}_{e\mu}^{V5}$ for $A \approx \pm 1$. For couplings that are not aligned to the SM, i.e., not “ $V - A$ ”, the dominant constraints on LDVs lighter than about 5 MeV are set by the Jodidio experiment, which limits UV scales of the order of 10^{10} GeV. Heavier LDVs are constrained only by TWIST, setting limits of the order of few $\times 10^9$ GeV. LDVs with “ $V - A$ ” couplings are constrained by TWIST with bounds of the same order, exceeding the corresponding Jodidio limits also in the light-mass regime.

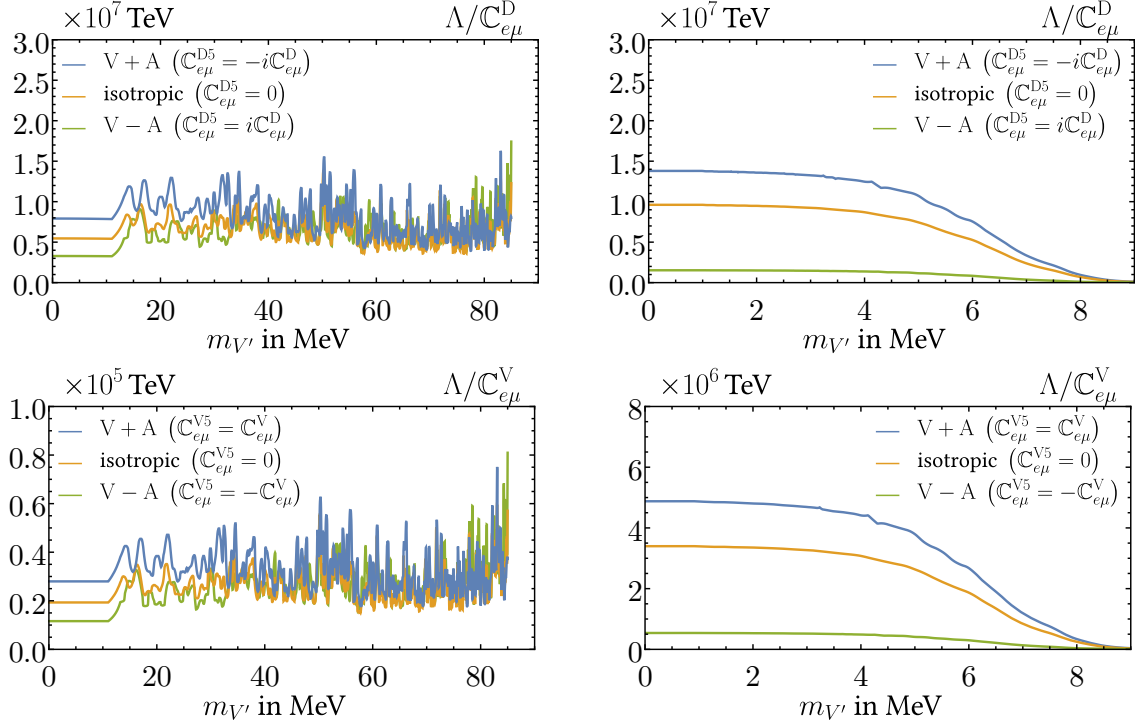


Figure 4: *Upper panel:* Lower limits on the dipole coupling for $\mu \rightarrow e$ transitions $\Lambda/|\mathbb{C}_{e\mu}^D|$ from TWIST [41] (left panel) and Jodidio et al. [18, 73] (right panel). The bounds are shown for three different choices for $\mathbb{C}_{e\mu}^{D5}$, corresponding to different angular distributions of the electron momentum, cf. Eq. (4.1): isotropic decay ($A = 0$), alignment to SM decay “ $V-A$ ” ($A = -1$) and “ $V+A$ ” ($A = +1$). *Lower panel:* same for the vector coupling $\Lambda/|\mathbb{C}_{e\mu}^V|$. See text for details.

$\tau \rightarrow \mu/e$ Transitions The limits from Belle II on $\tau \rightarrow \mu/e + \text{invis.}$ decays constrain $\tau \rightarrow e$ and $\tau \rightarrow \mu$ transitions according to Fig. 5, where we show the bounds on the dipole $\Lambda/\mathbb{C}_{\tau\ell}^D$ (left panel) and vector couplings $\Lambda/\mathbb{C}_{\tau\ell}^V$ (right panel). Constraints on the axial couplings $\Lambda/\mathbb{C}_{\tau\ell}^{D5}$ and $\Lambda/\mathbb{C}_{\tau\ell}^{V5}$ are at the same level, as the difference is suppressed by m_ℓ/m_τ , cf. Appendix E.5. Bounds for $\tau \rightarrow e$ and $\tau \rightarrow \mu$ transitions are comparable, limiting UV scales of the order of few $\times 10^7$ GeV for dipole couplings, and few $\times 10^6$ GeV for vector couplings.

5 Flavor-violating LDVs from the Renormalization Group

In this section we study the phenomenologically interesting scenario in which LDV interactions with the SM are flavor-universal in the UV theory, so that flavor-violating couplings are generated only from the SM flavor violation via the renormalization-group evolution. We start right below the UV scale Λ —taken to be much above the electroweak scale—and consider $SU(2)_L \times U(1)_Y$ invariant vector and dipole interactions of the V' to the SM. For vector couplings see the trivial $SU(2)_L \times U(1)_Y$ generalization of Eq. (2.3) and for dipole couplings see Eq. (2.6). We align possible new sources of flavor-violation of the V' with the flavor violation in the SM by taking the vector couplings to be flavor-universal, i.e., proportional to the identity matrix in flavor space, and by taking the dipole couplings to be proportional to the SM Yukawas. In both cases they are flavor diagonal in the mass basis, such that flavor-changing interactions with the V' are only induced by the renormalization-group evolution to

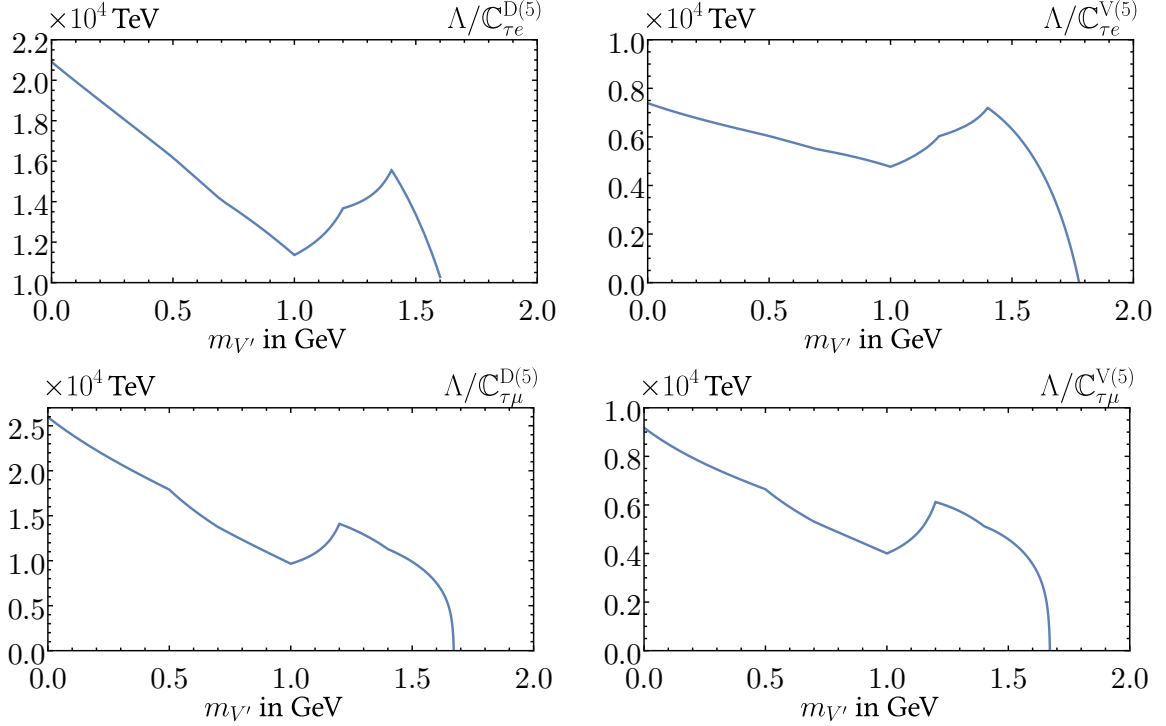


Figure 5: *Upper panel:* Lower limits on the dipole (left panel) and vector (right panel) couplings for $\tau \rightarrow e$ transitions $\Lambda/|C_{\tau e}^D|$, $\Lambda/|C_{\tau e}^V|$ from Belle II [38]. *Lower panel:* same for $\tau \rightarrow \mu$ transitions $\Lambda/|C_{\tau \mu}^D|$, $\Lambda/|C_{\tau \mu}^V|$. Constraints on the axial couplings $\Lambda/|C_{\tau \ell}^{D(5)}|$ and $\Lambda/|C_{\tau \ell}^{V(5)}|$ are essentially of the same size, as the difference is suppressed by m_ℓ/m_τ , cf. Appendix E.5.

the EW scale and always proportional to the CKM matrix. Flavor-violating couplings in the IR thus follow the paradigm of minimal flavor violation (MFV) [42].

We do not explicitly consider kinetic mixing between the $U(1)'$ LDV and the $U(1)_Y$ boson, as it leads only to a shift in the flavor-universal LDV couplings after diagonalising the photon kinetic terms. By working in this basis, our results also apply to models with kinetic mixing, upon re-defining the flavor-universal couplings.

We discuss separately the case of dipole and vector couplings in Section 5.1 and 5.2, respectively.

5.1 Dipole interactions

In the interaction basis, the dipole interactions of the LDV with SM fermions are given by (cf. Eq. (2.6))

$$\mathcal{L}_{\text{int}} \supset - \left(\bar{Q} Y_u \tilde{H} u_R + \bar{Q} Y_d H d_R + \text{h.c.} \right) + \frac{1}{\Lambda_6^2} V'_{\mu\nu} \left(\bar{Q} C_u^D \sigma^{\mu\nu} \tilde{H} u_R + \bar{Q} C_d^D \sigma^{\mu\nu} H d_R + \text{h.c.} \right), \quad (5.1)$$

with the SM Yukawa matrices Y_f , $f = u, d$, and arbitrary 3×3 matrices C_f^D . The one-loop RG equations for the couplings C_f^D and the Yukawa matrices Y_f are listed in Appendix B. For the UV universal setup that we consider, the initial conditions at the UV scale Λ_6 are

$$C_d^D|_{\mu=\Lambda_6} = c_d^D Y_d|_{\mu=\Lambda_6}, \quad C_u^D|_{\mu=\Lambda_6} = c_u^D Y_u|_{\mu=\Lambda_6}, \quad (5.2)$$

$i - j$	2 - 1	1 - 2	2 - 3	3 - 2	1 - 3	3 - 1
$(\mathbb{C}_u^{\text{DR}})_{i \neq j} / \Lambda$	$\lambda^5 y_b^2 y_c$	$\lambda^5 y_b^2 y_c$	$\lambda^2 y_b^2 y_t$	$\lambda^2 y_b^2 y_t$	$\lambda^3 y_b^2 y_t$	$\lambda^3 y_b^2 y_t$
$(\mathbb{C}_d^{\text{DR}})_{i \neq j} / \Lambda$	$\lambda^5 y_t^2 y_s$	$\lambda^5 y_t^2 y_s$	$\lambda^2 y_t^2 y_b$	$\lambda^2 y_t^2 y_b$	$\lambda^3 y_t^2 y_b$	$\lambda^3 y_t^2 y_b$

Table 3: Parametric size of leading flavor-violating contributions at low-energy in the UV universal scenario for dipole couplings, cf. Eq. (5.3). Here $\lambda \approx 0.23$ denotes the Wolfenstein parameter and $y_f = m_f/v$ are SM Yukawas couplings. Up-quark transitions (first line) are proportional to the high-scale coupling c_d^{D} , down-quark transitions (second line) are proportional to the high-scale coupling c_u^{D} , and all entries are multiplied by $v/\Lambda_6^2 \log(\Lambda_6/\mu)/(16\pi^2)$.

with $c_f^{\text{D}} \in \mathbb{C}$. By solving the RGE at leading-logarithmic accuracy and subsequently rotating to the mass basis for the quarks we find the low-energy dipole couplings in the L/R notation of Eq. (2.3) with $f = u, d$ to be⁴

$$\begin{aligned} \frac{1}{\Lambda} \mathbb{C}_u^{\text{DR}}(\mu) &= \frac{v}{\Lambda_6^2} \left(c_u^{\text{D}} \hat{Y}_u - \frac{1}{16\pi^2} \left(3c_u^{\text{D}} \hat{Y}_u \hat{Y}_u^\dagger \hat{Y}_u - c_d^{\text{D}} V_{\text{CKM}} \hat{Y}_d \hat{Y}_d^\dagger V_{\text{CKM}}^\dagger \hat{Y}_u \right) \log(\Lambda_6/\mu) \right), \\ \frac{1}{\Lambda} \mathbb{C}_d^{\text{DR}}(\mu) &= \frac{v}{\Lambda_6^2} \left(c_d^{\text{D}} \hat{Y}_d - \frac{1}{16\pi^2} \left(3c_d^{\text{D}} \hat{Y}_d \hat{Y}_d^\dagger \hat{Y}_d - c_u^{\text{D}} V_{\text{CKM}}^\dagger \hat{Y}_u \hat{Y}_u^\dagger V_{\text{CKM}} \hat{Y}_d \right) \log(\Lambda_6/\mu) \right), \end{aligned} \quad (5.3)$$

where V_{CKM} is the CKM matrix, and $\hat{Y}_f = m_f/v$ are the diagonal SM Yukawas. The left-handed couplings \mathbb{C}_f^{DL} are related to the ones in Eq. (5.3) by hermitian conjugation, $\mathbb{C}_f^{\text{DL}} = (\mathbb{C}_f^{\text{DR}})^\dagger$. Note that indeed flavor off-diagonal entries are generated in both the up- and the down-quark sector at one-loop. They are proportional to the CKM matrix and the UV coupling of the other sector, i.e., $\mathbb{C}_u^{\text{DR}} \propto c_d^{\text{D}}$ and $\mathbb{C}_d^{\text{DR}} \propto c_u^{\text{D}}$. Carrying out the matrix multiplications, one can identify the numerically leading contribution to a given flavor transition. We show these leading contributions in Table 3 for both sectors.

Using these results, we determine the experimental limits on the high-scale couplings c_d^{D} and c_u^{D} in Eq. (5.2) from the limits on two-body meson decays discussed in Section 3. Note that the renormalization scale μ is set to the EW scale since below there is no Yukawa running.

As expected from the high-level of flavor suppression inherent to the setup, the resulting bounds are very mild and often weaker than the constraints from perturbative unitarity. For this reason we only display in Fig. 6 (left panel) the strongest bounds, which come from $B \rightarrow K^*$ and require $\Lambda_6 \sim \text{TeV}$ for $c_u^{\text{D}} = 1$ (for $c_d^{\text{D}} = 1$ the limit on Λ_6 is far below the electroweak scale and is therefore not shown).

5.2 Vector interaction

In the interaction basis, the vector interactions of the LDV with the SM fermions are given by (cf. Eq. (2.3))

$$\mathcal{L}_{\text{int}} \supset - \left(\bar{Q} Y_u \tilde{H} u_R + \bar{Q} Y_d H d_R + \text{h.c.} \right) + V_\mu' \left(\bar{Q} C_Q^{\text{V}} \gamma^\mu Q + \bar{u}_R C_u^{\text{V}} \gamma^\mu u_R + \bar{d}_R C_d^{\text{V}} \gamma^\mu d_R \right), \quad (5.4)$$

with SM Yukawa matrices Y_f , $f = u, d$, and arbitrary hermitian 3×3 matrices C_X^{V} with $X = Q, u, d$. The one-loop RG equations for the couplings C_X^{V} and the Yukawa matrices Y_f are listed in Appendix B.

⁴Since the couplings at the UV scale Λ_6 are aligned to the SM Yukawa matrices, a correction from the Yukawa RGE, given in Appendix B, must be included.

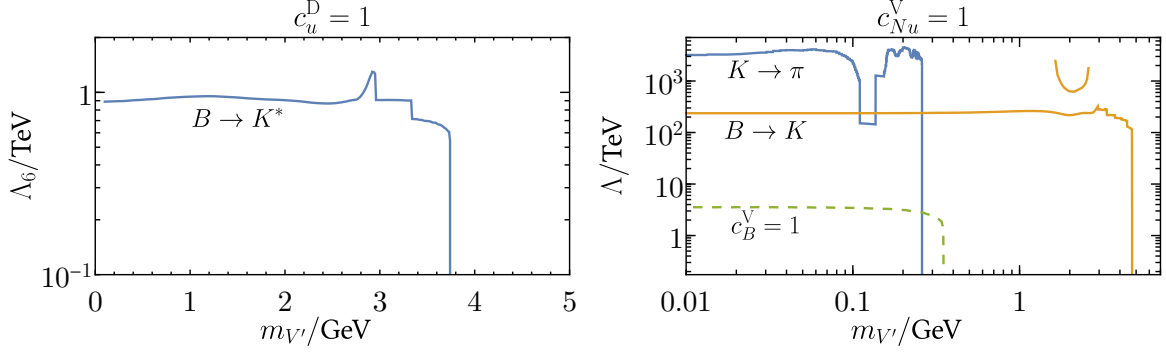


Figure 6: Lower limits on the UV scale in the UV universal scenario for dipole (left panel) and vector couplings (right panel), only showing the strongest constraints. See text for details.

For the UV universal setup that we consider in this section, the boundary conditions at the UV scale Λ are

$$C_Q^V(\Lambda) = c_Q^V \mathbb{1}_3, \quad C_u^V(\Lambda) = c_u^V \mathbb{1}_3, \quad C_d^V(\Lambda) = c_d^V \mathbb{1}_3. \quad (5.5)$$

with c_X^V real numbers.

By solving the RGE at leading-logarithmic accuracy and subsequently rotating to the mass basis for the quarks, we find the low-energy vector couplings in the L/R notation of Eq. (2.3) to be

$$\begin{aligned} \left(\frac{m_{V'}}{\Lambda}\right) \mathbb{C}_u^{\text{VL}}(\mu) &= c_Q^V \mathbb{1}_3 - \frac{1}{16\pi^2} \left((c_Q^V - c_u^V) \hat{Y}_u \hat{Y}_u^\dagger + (c_Q^V - c_d^V) V_{\text{CKM}} \hat{Y}_d \hat{Y}_d^\dagger V_{\text{CKM}}^\dagger \right) \log(\Lambda/\mu), \\ \left(\frac{m_{V'}}{\Lambda}\right) \mathbb{C}_d^{\text{VL}}(\mu) &= c_Q^V \mathbb{1}_3 - \frac{1}{16\pi^2} \left((c_Q^V - c_u^V) V_{\text{CKM}}^\dagger \hat{Y}_u \hat{Y}_u^\dagger V_{\text{CKM}} + (c_Q^V - c_d^V) \hat{Y}_d \hat{Y}_d^\dagger \right) \log(\Lambda/\mu), \\ \left(\frac{m_{V'}}{\Lambda}\right) \mathbb{C}_u^{\text{VR}}(\mu) &= c_u^V \mathbb{1}_3 - \frac{1}{8\pi^2} (c_u^V - c_Q^V) \hat{Y}_u^\dagger \hat{Y}_u \log(\Lambda/\mu), \\ \left(\frac{m_{V'}}{\Lambda}\right) \mathbb{C}_d^{\text{VR}}(\mu) &= c_d^V \mathbb{1}_3 - \frac{1}{8\pi^2} (c_d^V - c_Q^V) \hat{Y}_d^\dagger \hat{Y}_d \log(\Lambda/\mu), \end{aligned} \quad (5.6)$$

where V_{CKM} is the CKM matrix and $\hat{Y}_f = m_f/v$, $f = u, d$ are the diagonal SM Yukawas. Note that the couplings of right-handed interactions $\mathbb{C}_u^{\text{VR}}, \mathbb{C}_d^{\text{VR}}$ are always flavor diagonal, while flavor-violating terms in the IR are induced in the left-handed interactions $\mathbb{C}_u^{\text{VL}}, \mathbb{C}_d^{\text{VL}}$ proportionally to $c_Q^V - c_u^V$ and $c_Q^V - c_d^V$. Therefore, if the UV couplings are also universal among the different sectors, i.e., $c_Q^V = c_u^V = c_d^V$, there is no flavor violation in the IR at one-loop, as in this case the LDV actually couples to the baryon-number current, which is conserved at tree-level inducing flavor violation only at two-loop [74].

We now discuss this fact in more detail, before turning to the limits. One can rewrite the interactions in Eq. (5.4) for the case of flavor-universal UV boundary conditions in Eq. (5.5) in terms of the tree-level conserved (but anomalous) $U(1)_B$ current $J_B^\mu = \sum_i (\bar{Q}_i \gamma^\mu Q_i + \bar{u}_{Ri} \gamma^\mu u_{Ri} + \bar{d}_{Ri} \gamma^\mu d_{Ri})$, and the two non-conserved currents $J_{Nd}^\mu = \sum_i \bar{d}_{Ri} \gamma^\mu d_{Ri}$, and $J_{Nu}^\mu = \sum_i \bar{u}_{Ri} \gamma^\mu u_{Ri}$. As all currents are not conserved beyond tree-level, we take their coefficients to be proportional to the LDV mass

$$\mathcal{L}_{\text{int}} \supset - \left(\bar{Q} Y_u \tilde{H} u_R + \bar{Q} Y_d H d_R + \text{h.c.} \right) + \frac{m_{V'}}{\Lambda} V'_\mu \left[C_B^V J_B^\mu + C_{Nd}^V J_{Nd}^\mu + C_{Nu}^V J_{Nu}^\mu \right], \quad (5.7)$$

Matching to Eqs. (5.4) and (5.5) gives

$$\frac{m_{V'}}{\Lambda} c_B^V = c_Q^V, \quad \frac{m_{V'}}{\Lambda} c_{Nd}^V = c_d^V - c_Q^V, \quad \frac{m_{V'}}{\Lambda} c_{Nu}^V = c_u^V - c_Q^V. \quad (5.8)$$

$i - j$	2 - 1	3 - 2	3 - 1
$(\mathbb{C}_u^{\text{VL}})_{i \neq j}$	$\lambda^5 y_t^2$	$\lambda^2 y_t^2$	$\lambda^3 y_t^2$
$(\mathbb{C}_d^{\text{VL}})_{i \neq j}$	$\lambda^5 y_b^2$	$\lambda^2 y_b^2$	$\lambda^3 y_b^2$

Table 4: Parametric size of leading flavor-violating contributions to the low-energy vector couplings of V' in the UV universal scenario, cf. Eq. (5.6). Here $\lambda \approx 0.23$ denotes the Wolfenstein parameter. Up-quark transitions (first line) are proportional to the high-scale coupling $c_u^V - c_Q^V = c_{Nu}^V$, down-quark transitions (second line) are proportional to the high-scale coupling $c_d^V - c_Q^V = c_{Nd}^V$, and all entries are multiplied by $\log(\Lambda/\mu)/(16\pi^2)$.

At the one-loop level there is no flavor violation proportional to C_B^V . However, flavor violation does arise due to the non-conserved currents and is thus proportional to the difference of couplings $c_Q^V - c_u^V$ and $c_Q^V - c_d^V$. Rewriting Eq. (5.6) in terms of the UV coefficients $c_B^V, c_{Nd}^V, c_{Nu}^V$ with the proper LDV mass scaling gives finally

$$\begin{aligned}
\left(\frac{m_{V'}}{\Lambda}\right) \mathbb{C}_u^{\text{VL}}(\mu) &= \frac{m_{V'}}{\Lambda} \left[c_B^V \mathbb{1}_3 + \frac{1}{16\pi^2} \left(c_{Nu}^V \hat{Y}_u \hat{Y}_u^\dagger + c_{Nd}^V V_{\text{CKM}}^V \hat{Y}_d \hat{Y}_d^\dagger V_{\text{CKM}}^\dagger \right) \log(\Lambda/\mu) \right], \\
\left(\frac{m_{V'}}{\Lambda}\right) \mathbb{C}_d^{\text{VL}}(\mu) &= \frac{m_{V'}}{\Lambda} \left[c_B^V \mathbb{1}_3 + \frac{1}{16\pi^2} \left(c_{Nu}^V V_{\text{CKM}}^\dagger \hat{Y}_u \hat{Y}_u^\dagger V_{\text{CKM}} + c_{Nd}^V \hat{Y}_d \hat{Y}_d^\dagger \right) \log(\Lambda/\mu) \right], \\
\left(\frac{m_{V'}}{\Lambda}\right) \mathbb{C}_u^{\text{VR}}(\mu) &= \frac{m_{V'}}{\Lambda} \left[(c_B^V + c_{Nu}^V) \mathbb{1}_3 - \frac{1}{8\pi^2} c_{Nu}^V \hat{Y}_u \hat{Y}_u^\dagger \log(\Lambda/\mu) \right], \\
\left(\frac{m_{V'}}{\Lambda}\right) \mathbb{C}_d^{\text{VR}}(\mu) &= \frac{m_{V'}}{\Lambda} \left[(c_B^V + c_{Nd}^V) \mathbb{1}_3 - \frac{1}{8\pi^2} c_{Nd}^V \hat{Y}_d \hat{Y}_d^\dagger \log(\Lambda/\mu) \right], \tag{5.9}
\end{aligned}$$

The numerically leading contributions to a given (hermitian) flavor transition in left-handed interactions are shown in Table 4 for both sectors. We display the resulting bounds on Λ in the right panel of Fig. 6 for $c_{Nu}^V = 1$ (there is no constraint from c_{Nd}^V at one-loop), which are of order $\Lambda \geq 10^3$ TeV for $K \rightarrow \pi$ transitions. These limits are weakened by about an order of magnitude for LDV masses above $m_K - m_\pi$, where the dominant constraint comes from $B \rightarrow K$ transitions. In dashed green, we also show the limits coming from the flavor-violating contribution that is induced at the two-loop level by the coupling of the LDV to the anomalous baryon current J_B^μ . The corresponding limit on the scale Λ has been obtained by rescaling the result for $K \rightarrow \pi$ of Fig. (1) from Ref. [74], giving $\Lambda \geq 3.5$ TeV for $c_B^V = 1$ and $c_{Nu}^V = c_{Nd}^V = 0$. This is about three orders of magnitude weaker than the limit one obtains if the LDV also couples to currents that are not conserved at tree-level, i.e., taking $c_{Nu}^V = c_{Nd}^V = 1$.

6 Summary and Conclusions

In this work we have systematically studied the flavor phenomenology of light dark vectors (LDVs). We have restricted our analysis to scenarios where the LDV is directly linked to dark matter, and is either itself invisible or promptly decays to invisible particles, such that the LDV appears as missing energy. Working in the context of a general EFT, we have considered both flavor-violating dipole (see Eq. (2.1)) and vector couplings (see Eq. (2.2)) of the LDV to SM fermions. We have calculated the resulting predictions for the decay rates of mesons, baryons, and polarized leptons as a function of the LDV mass, see Section E. These predictions were compared to the experimental limits on various hadronic processes (Table 1) and LFV transitions (Table 2). For $B \rightarrow \pi/K/K^*$ decays experimental

limits from B-factories are only available for three-body decays with two invisible neutrinos, so we have recasted available data to obtain bounds on the two-body decay with missing energy as a function of the LDV mass, see Fig. 7. The resulting limits on general vector and dipole interactions of the LDV are summarized in Figs. 2 and 3 for the quark sector, and in Fig. 4 and 5 for the lepton sector. Vector couplings are at least dimension-five operators, which results in very stringent limits on the UV scale, reaching up to 10^{12} GeV in $K \rightarrow \pi$ decays, 10^8 GeV in B - and D -meson decays, 10^9 GeV in $\mu \rightarrow e$ decays, and 10^7 GeV in $\tau \rightarrow \mu/e$ decays. Bounds on dipole couplings are weaker, if viewed as dimension-six operators above the EW scale, but they still probe UV scales of order 10^6 GeV in $K \rightarrow \pi$ and $\mu \rightarrow e$ decays. Importantly, all channels will be improved by present or near-future experiments, such as NA62, Belle II, BES III, MEG-II or Mu3e. We have also discussed a scenario where couplings in the UV are flavor-universal, so that quark-flavor violation is only induced radiatively through the CKM matrix. For this analysis we derived the relevant renormalization-group equations (RGEs) for both dipole and minimal couplings in Appendix B, and used our previous results to convert limits on flavor-changing interactions into limits on flavor-diagonal couplings, see Figure. 6.

To summarize, the aim of this work is to stress the importance of flavor-violating transitions for light, dark-matter searches, which is copiously produced in the lab as missing energy in decays of SM particles. Here we focused on the LDV as part of a dark sector, and showed that present constraints from precision flavor experiments already probe UV scales as large as 10^{12} GeV. This underlines the important role of present and next-generation flavor factories in hunting down dark matter in the laboratory.

Acknowledgments

We would like to thank Adam Falkowski, Jorge Martin Camalich and Zhijun Li for useful discussions and Jure Zupan for comments on the manuscript. This work has received support from the European Union’s Horizon 2020 research and innovation programme under the Marie Skłodowska-Curie grant agreement No 860881-HIDDeN and is partially supported by project B3a and C3b of the DFG-funded Collaborative Research Center TRR257 “Particle Physics Phenomenology after the Higgs Discovery”.

A UV Motivation of Vector Couplings

In this section we motivate the scaling behavior of the flavor-violating vector coupling in the Lagrangian of Eq. (2.2), both by EFT considerations and explicit UV-complete models. In perturbative UV completions, the scaling is at least linear in the dark $U(1)'$ breaking scale, and we will provide two example scenarios: one that gives linear and one that gives quadratic scaling. We begin with the EFT discussion of the latter.

A.1 EFT Discussion for Quadratic scaling

For the EFT approach it is convenient to consider the coupling to the Goldstone boson G in the gaugeless limit, rather than the coupling of the dark vector V'_μ itself. They are related by the Goldstone-boson Equivalence Theorem, which states that at sufficiently high energies, or equivalently sufficiently small dark vector masses $m'_{V'}$, the vector boson coupling is dominated by its longitudinal polarization, which in the small $m'_{V'}$ limit becomes the Goldstone boson. Thus one can work out the couplings of the Goldstone boson and recover the relevant vector-boson couplings by replacing $\partial_\mu G \rightarrow -m_{V'} V'_\mu$ in the interaction Lagrangian.

We, therefore, consider the case where the dark $U(1)'$ gauge group is spontaneously broken by some (SM singlet) scalar field S with charge $+1$ under the $U(1)'$. We take the gauge-less limit, so that G is a true Goldstone boson, contained in S according to

$$S = \frac{v'}{\sqrt{2}} \exp(iG/v'), \quad (\text{A.1})$$

where $v'/\sqrt{2}$ is the (real) VEV that breaks $U(1)'$, connected to the dark vector mass by $m_{V'} = g'v'$, and we have ignored the radial mode that obtains its mass around v' . This mode, together with all UV fields are taken to be much heavier than the electroweak scale, so that in the IR there is only the SM and the Goldstone boson $G \subset S$, which is formally invariant under global $U(1)'$ transformations treating S as a spurion with charge $+1$. Note that one can always realize such a scenario by making g' sufficiently small. Writing down the general EFT for this setup, it is clear that if SM fields are not charged under $U(1)'$, the possible couplings of the Goldstone to SM fields must involve the same powers of S^\dagger and S . The first such bilinear that gives a non-trivial combination containing the Goldstone is then $S^\dagger \overleftrightarrow{\partial}_\mu S \supset iv' \partial_\mu G$. This implies that, e.g., right-handed down quarks can only couple to the Goldstone at the level of dimension-six operators only

$$\mathcal{L}_{\text{quadratic}}^{\text{EFT}} \supset \frac{c_{ij}}{\Lambda^2} (iS^\dagger \overleftrightarrow{\partial}_\mu S) (\bar{d}_{Ri} \gamma^\mu d_{Rj}) = -\frac{c_{ij}}{\Lambda^2} v' \partial_\mu G (\bar{d}_{Ri} \gamma^\mu d_{Rj}), \quad (\text{A.2})$$

where Λ is the UV scale and in general there is flavor violation in the (hermitian) EFT coefficients, $c_{i \neq j} \neq 0$. The coupling of the dark vector in this setup is then recovered by $\partial_\mu G \rightarrow -m_{V'} V'_\mu$, so is given by

$$\mathcal{L}_{\text{quadratic}}^{\text{EFT}} \supset c_{ij} \frac{v' m'_{V'}}{\Lambda^2} V'_\mu (\bar{d}_{Ri} \gamma^\mu d_{Rj}). \quad (\text{A.3})$$

This analysis demonstrates that the interactions of dark vectors with SM fields that are neutral under the $U(1)'$ scale at least as $m'_{V'}/\Lambda \times v'/\Lambda$. In particular they involve an additional factor of the $U(1)'$ breaking scale as compared to Eq. (2.2). Below we will confirm this expectation in an explicit UV model, see Section A.3.

A.2 EFT Discussion for Linear scaling

In order to have dark-vector couplings with a linear scaling in the $U(1)'$ breaking scale, one necessarily has to charge SM fields under $U(1)'$. In this case the vector boson couples directly to the charged fields via the dimension-four operator, e.g., for right-handed down quarks

$$\mathcal{L}_{\text{linear}} \supset g' V'_\mu (\bar{d}_R \gamma^\mu X_d d_R). \quad (\text{A.4})$$

where X_d is the diagonal $U(1)'$ charge matrix. To see how off-diagonal entries are generated, one has to rotate to the mass basis, which is governed by the Yukawa couplings. It is clear that there is no flavor violation if X_d is universal, i.e., proportional to the identity matrix. If instead charges are non-universal, the mass matrix cannot be generic at the renormalizable level, i.e., it does not yield realistic fermion masses without breaking $U(1)'$. Therefore, insertions of S or S^\dagger have to be considered to obtain realistic fermion masses.

Restricting for simplicity to two generations, and charging only d_{R1} with charge $+1$, i.e., $X_d = \text{Diag}(1, 0)$, $X_Q = X_H = 0$, the full Yukawa matrix requires higher-dimensional operators to have full rank

$$\mathcal{L}_{\text{linear}}^{\text{EFT}} \supset -y_i \bar{Q}_i H d_{R2} - z_i \frac{S^\dagger}{\Lambda} \bar{Q}_i H d_{R1} + \text{h.c.} \quad (\text{A.5})$$

Thus the down-quark Yukawa matrix is given by

$$Y_d = \begin{pmatrix} z_1 \epsilon & y_1 \\ z_2 \epsilon & y_2 \end{pmatrix} \quad \text{with} \quad \epsilon = \frac{v'}{\sqrt{2}\Lambda} \quad (\text{A.6})$$

We can ignore here the Goldstone in S , since we already have the coupling of the gauge field in Eq. (A.4), which leads to flavor-violating couplings with V' after rotating to the mass basis. Nevertheless we can also reproduce this coupling with the same arguments as above: in the gauge-less limit, we rescale $d_{R1} \rightarrow d_{R1} e^{iG/v'}$, which removes G from the Yukawa sectors. Ignoring chiral anomalies, this rescaling only affects the kinetic terms, as it is a *local* $U(1)'$ transformation

$$\mathcal{L}_{\text{linear}}^{\text{EFT}} \supset i \bar{d}_{R1} \not{\partial} d_{R1} \rightarrow -\frac{\partial_\mu G}{v'} \bar{d}_{R1} \gamma^\mu d_{R1}, \quad (\text{A.7})$$

which reproduces Eq. (A.4) upon $\partial_\mu G \rightarrow -m_{V'} V_\mu = -g' v' V_\mu$.

We are left to diagonalize the Yukawa matrix Y_d in Eq. (A.6), or rather $Y_d^\dagger Y_d$, in order to find the mixing matrix V_d of right-handed down quarks, defined as $V_Q^\dagger Y_d V_d = Y_d^{\text{diag}}$. In the limit when $\epsilon \ll 1$, one has

$$V_d \approx \begin{pmatrix} 1 & z_2/y_2 \epsilon \\ -z_2/y_2 \epsilon & 1 \end{pmatrix}, \quad (\text{A.8})$$

where we have set $y_1 = 0$ without loss of generality. Rotating the dark-vector couplings in Eq. (A.4) to the mass basis defined by $d_R \rightarrow V_d d_R$ gives finally

$$\mathcal{L}_{\text{linear}} \supset g' V'_\mu \left(\bar{d}_R \gamma^\mu V_d^\dagger X_d V_d d_R \right) = g' V'_\mu (V_d^*)_{1i} (V_d)_{1j} \left(\bar{d}_{Ri} \gamma^\mu d_{Rj} \right), \quad (\text{A.9})$$

so that indeed off-diagonal couplings are generated proportional to $g' (V_d^*)_{11} (V_d)_{12} \sim g' \epsilon \sim m_{V'}/\Lambda$.

To summarize, we have demonstrated that vector interactions of dark vectors can indeed be proportional to a single power of the $U(1)'$ breaking, and thus scale with the dark-vector mass as in Eq. (A.4), if SM fermions have non-universal $U(1)'$ charges. This situation is quite generic in models where SM Yukawa hierarchies are explained by non-anomalous abelian flavor symmetries, for example simple $U(1)_F$ Froggatt-Nielsen models [51], see e.g. Refs. [7] for examples of such models without extra heavy fermions to cancel anomalies. It is well-known how to build UV completions for such models [75, 76], and below in Section A.4 we will present an illustrative example.

A.3 Explicit UV Model for Quadratic scaling

We first construct an explicit renormalizable model for the scaling of vector interactions in Eq. (2.2) quadratic in the dark $U(1)'$ breaking scale. We restrict the discussion for simplicity to the down-quark sector with two generations. The field content is summarized in Table 5, and is clearly anomaly-free.

	Q_i	d_{Ri}	H	S	ψ_{Li}	ψ_{Ri}
$SU(2)_L$	2	1	2	1	1	1
$U(1)_Y$	1/6	-1/3	1/2	0	-1/3	-1/3
$U(1)'$	0	0	0	1	-1	-1

Table 5: Field content of a renormalizable model featuring quadratic scaling. We restrict the discussion to the down-quark sector with two generations for SM quarks and heavy vector-like fermions ψ_{Li} , ψ_{Ri} , with $i = 1, 2$ carrying $U(1)'$ charges in addition to the scalar S .

The Lagrangian reads

$$\mathcal{L} = \mathcal{L}_{\text{kinetic}} + \mathcal{L}_{\text{Yukawa}} + \mathcal{L}_{\text{scalar}} + \mathcal{L}_{\text{int-}V'}, \quad (\text{A.10})$$

with standard kinetic terms for all fields and

$$\mathcal{L}_{\text{Yukawa}} = -Y_{ij}^d \bar{Q}_i H d_{Rj} - m_\psi \bar{\psi}_{Li} \psi_{Ri} - \alpha_{ij} \bar{\psi}_{Li} d_{Rj} S^\dagger + \text{h.c.} \quad (\text{A.11})$$

$$\mathcal{L}_{\text{int-}V'} = -g' V'_\mu (\bar{\psi}_{Li} \gamma^\mu \psi_{Li} + \bar{\psi}_{Ri} \gamma^\mu \psi_{Ri}), \quad (\text{A.12})$$

$$\mathcal{L}_{\text{scalar}} = m_H^2 |H|^2 + m_S^2 |S|^2 - \lambda_H |H|^4 - \lambda_S |S|^4 - \lambda_{HS} |H|^2 |S|^2. \quad (\text{A.13})$$

For a suitable choice of parameters, the last part in $\mathcal{L}_{\text{scalar}}$ gives a vacuum expectation value to S , $\langle S \rangle = v'/\sqrt{2}$, which sets the mass of the dark vector boson to

$$m_{V'} = v' g', \quad (\text{A.14})$$

and induces a mixing between chiral quarks, d_R , and vector-like fermions, ψ , from the mixing term in $\mathcal{L}_{\text{Yukawa}}$. In the limit of $m_\psi \gg v' \gg v$ we can integrate out the vector-like fermions using their equations of motion neglecting their kinetic terms

$$\psi_{Ri} = -\frac{\alpha_{ij}}{m_\psi} d_{Rj} S^\dagger, \quad \psi_{Li} = 0. \quad (\text{A.15})$$

Plugging this back into kinetic terms and \mathcal{L}_{int} lead to the EFT

$$\mathcal{L}_{\text{int}} \supset -g' V'_\mu \frac{S^\dagger S}{m_\psi^2} C_{ij} (\bar{d}_{Ri} \gamma^\mu d_{Rj}) + \frac{S^\dagger S}{m_\psi^2} C_{ij} (i \bar{d}_{Ri} \not{\partial} d_{Rj}) + \frac{S i \partial_\mu S^\dagger}{m_\psi^2} C_{ij} (\bar{d}_{Ri} \gamma^\mu d_{Rj}), \quad (\text{A.16})$$

where $C_{ij} = (\alpha^\dagger \alpha)_{ij}$. Next we integrate out the radial mode by substituting S with the Goldstone parametrization in Eq. (A.1) and use the definition of the dark-vector mass to find

$$\mathcal{L}_{\text{int}} \supset -V'_\mu \frac{m_{V'} v'}{2m_\psi^2} C_{ij} (\bar{d}_{Ri} \gamma^\mu d_{Rj}) + \frac{(v')^2}{2m_\psi^2} C_{ij} (i \bar{d}_{Ri} \not{\partial} d_{Rj}) + \partial_\mu G \frac{v'}{2m_\psi^2} C_{ij} (\bar{d}_{Ri} \gamma^\mu d_{Rj}), \quad (\text{A.17})$$

recovering the gauge-invariant⁵ combination $V'_\mu - \partial_\mu G / m_{V'}$. Without loss of generality we can assume that Y_{ij}^d is diagonal, so that we are already in the mass basis. Nevertheless, we do need to re-diagonalize the kinetic terms due to the second term in Eq. (A.17) induced in the EFT. In the limit of $v' \ll m_\psi$ this is readily achieved by the rescaling $d_{Ri} \rightarrow d_{Ri} - (v')^2 / (4m_\psi^2) C_{ij} d_{Rj}$. This leads to additional small corrections of $\mathcal{O}(1/m_\psi^4)$ to the final dark-vector couplings, which can be neglected, such that the leading couplings from the first term in Eq. (A.17) remain

$$\mathcal{L}_{\text{quadratic}} = -\frac{m_{V'} v'}{2m_\psi^2} C_{ij} V'_\mu (\bar{d}_{Ri} \gamma^\mu d_{Rj}). \quad (\text{A.18})$$

These couplings are indeed quadratic in v' and are in general flavor violating, $C_{i \neq j} \neq 0$. This matches to the EFT term in Eq. (A.3) upon identifying $C_{ij} / m_\psi^2 = -2c_{ij} / \Lambda^2$.

⁵In our conventions $V'_\mu \rightarrow V'_\mu + \partial_\mu \beta / g'$, $S \rightarrow \exp(i\beta) S$, $G \rightarrow G + \beta v'$, $\psi \rightarrow \exp(-i\beta) \psi$.

A.4 Explicit UV Model for Linear scaling

We now construct an explicit renormalizable model for the minimal scaling of vector interactions in Eq. (2.2) proportional to a single power of the dark-vector mass. These types of models are motivated by scenarios addressing the SM flavor puzzle with non-anomalous abelian horizontal symmetries, see e.g. Ref. [7]. We restrict the discussion for simplicity to the down-quark sector with two generations. The field content is summarized in Table 6, and is *not* anomaly-free. However, we can always introduce further suitably charged chiral fermions in the right-handed up- and charged-lepton sector in order to cancel color and electromagnetic anomalies, respectively. Note that ψ_R and d_{R2} carry the same quantum numbers.

	Q_i	d_{R1}	d_{R2}	H	S	ψ_L	ψ_R
$SU(2)_L$	2	1	1	2	1	1	1
$U(1)_Y$	1/6	-1/3	-1/3	1/2	0	-1/3	-1/3
$U(1)'$	0	1	0	0	1	0	0

Table 6: Field content of a renormalizable model featuring linear scaling. We restrict the discussion to the down-quark sector with two generations for SM quarks and one family of heavy vector-like fermions ψ_L, ψ_R uncharged under $U(1)'$.

The Lagrangian reads

$$\mathcal{L} = \mathcal{L}_{\text{kinetic}} + \mathcal{L}_{\text{Yukawa}} + \mathcal{L}_{\text{scalar}} + \mathcal{L}_{\text{int-}V'}, \quad (\text{A.19})$$

with standard kinetic terms for all fields and

$$\mathcal{L}_{\text{Yukawa}} = -y_i \bar{Q}_i H d_{R2} - z_i \bar{Q}_i H \psi_R - m_\psi \bar{\psi}_L \psi_R - \alpha \bar{\psi}_L d_{R1} S^\dagger + \text{h.c.} \quad (\text{A.20})$$

$$\mathcal{L}_{\text{int-}V'} = g' V'_\mu \bar{d}_{R1} \gamma^\mu d_{R1}, \quad (\text{A.21})$$

$$\mathcal{L}_{\text{scalar}} = m_H^2 |H|^2 + m_S^2 |S|^2 - \lambda_H |H|^4 - \lambda_S |S|^4 - \lambda_{HS} |H|^2 |S|^2, \quad (\text{A.22})$$

where we have simply defined ψ_R to be that field having a mass term with ψ_L . This already gives Eq. (A.4) and the first term in Eq. (A.5) from the EFT discussion, so it only remains to show that integrating out ψ_L, ψ_R induces the second term in Eq. (A.5). The equations of motion for the heavy fermions read, neglecting kinetic terms

$$\bar{\psi}_L = -\frac{z_i}{m_\psi} \bar{Q}_i H, \quad \psi_R = -\frac{\alpha}{m_\psi} d_{R1} S^\dagger, \quad (\text{A.23})$$

and, therefore, the resulting EFT Lagrangian term is

$$\mathcal{L}_{\text{linear}} \supset \frac{z_i \alpha}{m_\psi} \bar{Q}_i H d_{R1} S^\dagger. \quad (\text{A.24})$$

This indeed reproduces Eq. (A.5) with the identification of the UV scale as $\Lambda = -m_\psi/\alpha$. The remaining calculation follows the EFT discussion, which shows that in these type of UV models the flavor violating couplings to V' scale indeed linearly with $m_{V'}/\Lambda$.

B Renormalization Group Equations

In this appendix we collect our results for the renormalization group equations relevant for the $SU(2)_L \times U(1)_Y$ interactions of the LDV with SM quarks as discussed in Section 5. Since in the current work we focused on the case of the UV universal scenario, in which flavor-violation originates only from the SM CKM matrix, we present here only the one-loop RGEs proportional to Yukawa couplings. However, in what follows the matrices C_u^D , C_d^D , C_Q^V , C_u^V , and C_d^D are generic matrices in flavor space, i.e., we have not assumed any alignment with the SM Yukawas. The relevant terms in the Lagrangian are the SM Yukawa interaction, the dipole, and the vector interactions with the LDV. They respectively read:

$$\mathcal{L}_{\text{Yukawa}} = -\bar{Q} Y_u \tilde{H} u_R - \bar{Q} Y_d H d_R + \text{h.c.}, \quad (\text{B.1})$$

$$\mathcal{L}_{\text{Dipole}} = \frac{1}{\Lambda^2} V'_{\mu\nu} \left(\bar{Q} C_u^D \sigma^{\mu\nu} \tilde{H} u_R + \bar{Q} C_d^D \sigma^{\mu\nu} H d_R + \text{h.c.} \right), \quad (\text{B.2})$$

$$\mathcal{L}_{\text{Vector}} = V'_\mu \left(\bar{Q} C_Q^V \gamma^\mu Q + \bar{u}_R C_u^V \gamma^\mu u_R + \bar{d}_R C_d^V \gamma^\mu d_R \right). \quad (\text{B.3})$$

The one-loop RGEs for Yukawa running read [77]

$$\begin{aligned} 16\pi^2 \frac{dY_u}{d \ln \mu} &= \frac{3}{2} \left(Y_u Y_u^\dagger Y_u - Y_d Y_d^\dagger Y_u \right) + n_c \text{Tr} \left[Y_u Y_u^\dagger + Y_d Y_d^\dagger \right] Y_u, \\ 16\pi^2 \frac{dY_d}{d \ln \mu} &= \frac{3}{2} \left(Y_d Y_d^\dagger Y_d - Y_u Y_u^\dagger Y_d \right) + n_c \text{Tr} \left[Y_u Y_u^\dagger + Y_d Y_d^\dagger \right] Y_d, \end{aligned} \quad (\text{B.4})$$

with $n_c = 3$ denoting the number of colors. The one-loop running of the Yukawas is relevant for the dipole analysis because the RG-evolved Yukawas contribute to the flavor-violating couplings upon rotation to the quark mass-eigenstates at the EW scale [78].

For the one-loop RGE of the dipole couplings proportional to the SM Yukawas we find

$$\begin{aligned} 16\pi^2 \frac{dC_u^D}{d \ln \mu} &= \frac{5}{2} Y_u Y_u^\dagger C_u^D - \frac{3}{2} Y_d Y_d^\dagger C_u^D - C_d^D Y_d^\dagger Y_u + 2C_u^D Y_u^\dagger Y_u \\ &\quad + n_c \text{Tr} \left[Y_u Y_u^\dagger + Y_d Y_d^\dagger \right] C_u^D, \\ 16\pi^2 \frac{dC_d^D}{d \ln \mu} &= \frac{5}{2} Y_d Y_d^\dagger C_d^D - \frac{3}{2} Y_u Y_u^\dagger C_d^D - C_u^D Y_u^\dagger Y_d + 2C_d^D Y_d^\dagger Y_d \\ &\quad + n_c \text{Tr} \left[Y_u Y_u^\dagger + Y_d Y_d^\dagger \right] C_d^D. \end{aligned} \quad (\text{B.5})$$

For the one-loop RGE of the vector couplings proportional to the SM Yukawas we find

$$\begin{aligned} 16\pi^2 \frac{dC_Q^V}{d \ln \mu} &= -Y_u C_u^V Y_u^\dagger - Y_d C_d^V Y_d^\dagger + \frac{1}{2} \left(Y_u Y_u^\dagger + Y_d Y_d^\dagger \right) C_Q^V + \frac{1}{2} C_Q^V \left(Y_u Y_u^\dagger + Y_d Y_d^\dagger \right), \\ 16\pi^2 \frac{dC_u^V}{d \ln \mu} &= -2Y_u^\dagger C_Q^V Y_u + Y_u^\dagger Y_u C_u^V + C_u^V Y_u^\dagger Y_u, \\ 16\pi^2 \frac{dC_d^V}{d \ln \mu} &= -2Y_d^\dagger C_Q^V Y_d + Y_d^\dagger Y_d C_d^V + C_d^V Y_d^\dagger Y_d. \end{aligned} \quad (\text{B.6})$$

C Recast of Experimental Limits

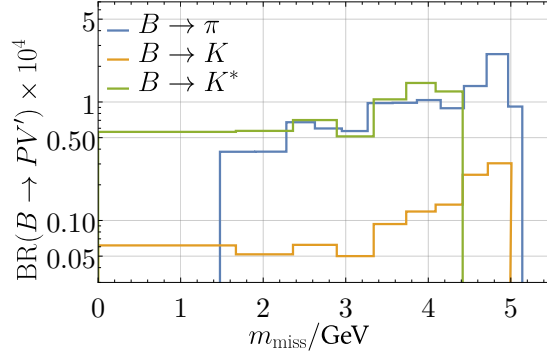


Figure 7: Upper 95 % CL_s limits on the two-body branching ratios $B \rightarrow K/K^*/\pi + V'$, as a function of the missing mass $m_{\text{miss}} = \sqrt{q^2}$, obtained by recasting the experimental three-body searches at BaBar [35, 36], see text for details.

Experimental collaborations often provide only limits on the $P \rightarrow P' + \text{invisible}$ branching ratios in terms of the three body decay $P \rightarrow P'\nu\bar{\nu}$, as a function of the squared invariant mass of the di-neutrino system q^2 . In order to get the experimental limits on the two body decays $P \rightarrow P'V$, we use the event count n_B per q^2 -bin information, if provided by the experimental collaborations. Only the BaBar experiment [35, 36] provides all information needed to perform a recast for two-body decays $B \rightarrow K/K^*/\pi + V$. For $B \rightarrow K^{(*)}$ and dark-vector masses $m_{V'} < 3 \text{ GeV}$, we use the sophisticated recast of Ref. [57], otherwise we estimate upper limits on the Wilson coefficients in terms of the CL_s method as explained below.

For a given Wilson coefficient C , the number of signal events s in a q^2 -bin i is given as

$$s = \text{BR}_{P \rightarrow P'}^i(C) \times N_{\text{tot}} \times \epsilon_i, \quad (\text{C.1})$$

where N_{tot} is the total number of P mesons and ϵ_i the efficiency associated to bin i . Further, $\text{BR}_{P \rightarrow P'}^i(C)$ denotes the branching ratio of $P \rightarrow P'$ within the q^2 -bin i . The $s + b$ likelihood is then given as a Poisson distribution in the number of signal plus background events. The efficiency ϵ_i and total number of P mesons N_{tot} are included as global observables associated to auxiliary measurements. The uncertainty on the signal, assumed to be Gaussian, is given by the NP theoretical prediction and is dominated by the form-factor uncertainty. The systematic uncertainty on the background is implemented as a Gaussian distribution. With this in mind, we denote the likelihood as $\mathcal{L}(x|C, \nu)$ with x being the outcome, i.e., the observed data, C the parameter of interest, i.e., the Wilson coefficient, and ν the nuisance parameters. As a test statistics t_C , we choose a one-sided profile likelihood. Note that the parameter of interest is actually $|C|^2$ since the branching ratio only depends on $|C|^2$ as we only consider one coupling at a time. The p -value p_C of the $s + b$ hypothesis for a given value of the Wilson coefficient C is then given by

$$p_C = \int_{t_C^{\text{obs}}}^{\infty} f(t_C|C, \hat{\nu}(C)) dt_C, \quad (\text{C.2})$$

where t_C^{obs} denotes the value of the test statistics for the observed data, f denotes the pdf of the test statistics t_C , and $\hat{\nu}(C)$ are the values of the nuisance parameter that maximise the likelihood for a

given C . The $\alpha\%$ CL_s limit on the Wilson coefficient is then given by the value of C such that

$$\frac{pC}{p_0} = 1 - \frac{\alpha}{100}, \quad (\text{C.3})$$

where p_0 denotes the p -value of the background only hypothesis. In order to evaluate Eq. (C.2), one needs the pdf f of the test statistics t_C for which we use the ROOT toolkit RooStats in order to sample the distribution by means of a Monte Carlo method.

Taking the $\text{BR}(P \rightarrow P'V)$ as a parameter of interest instead of the Wilson coefficient C , we can determine a model independent limit $\text{BR}_{\text{exp}}(P \rightarrow P'V)$ on the two body branching ratios, see Figure 7.

D Limits in the L/R Basis

In this appendix we present bounds on the couplings in the L/R basis $\{\mathbb{C}_{ij}^{\text{DR}}, \mathbb{C}_{ij}^{\text{DL}}, \mathbb{C}_{ij}^{\text{VR}}, \mathbb{C}_{ij}^{\text{VL}}\}$, which are obtained from the limits in the V/A basis (discussed in Section 3 and 4)) using Eq. (2.4). As the decay rates are symmetric with respect to $\mathbb{C}^{\text{L}} \leftrightarrow \mathbb{C}^{\text{R}}$ the bounds on both couplings are the same.

D.1 Quark Dipole Interactions

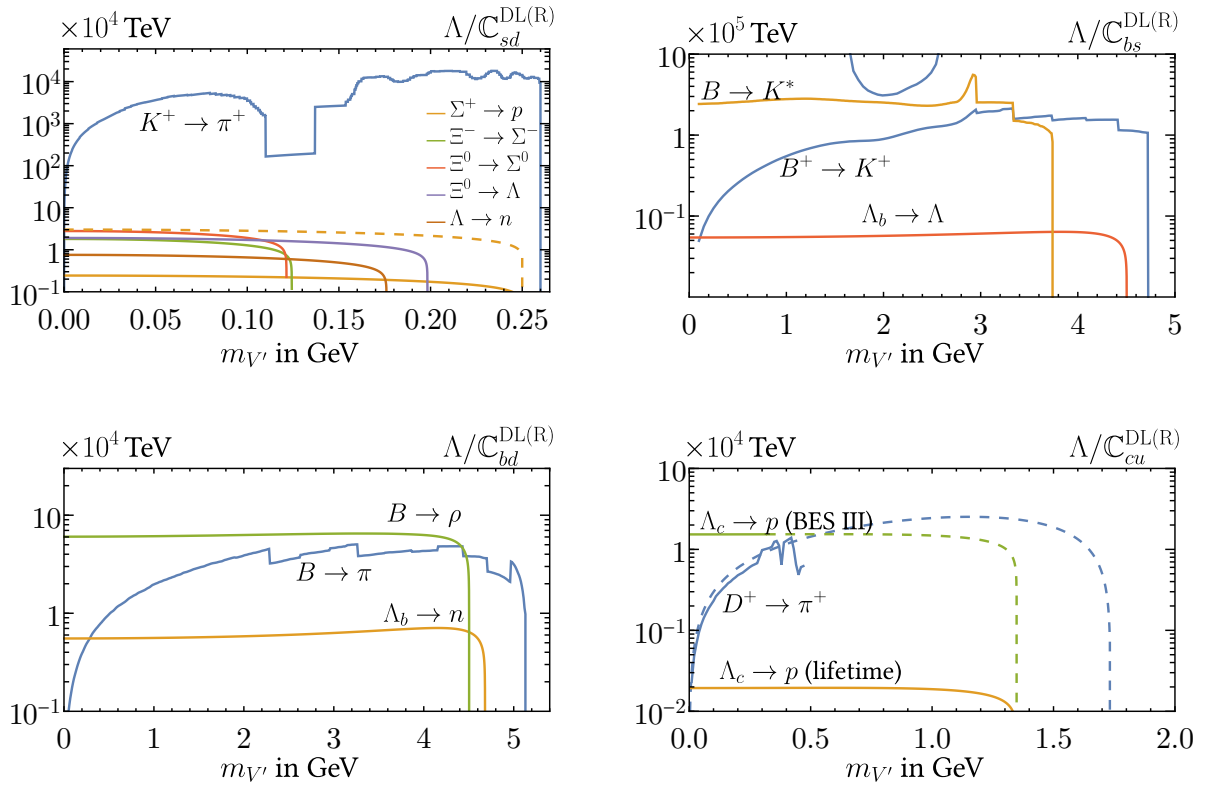


Figure 8: Upper limits on quark-flavor violating dipole couplings $\Lambda/|\mathbb{C}_{ij}^{\text{DL}}|$, for $s \rightarrow d, b \rightarrow s, b \rightarrow d$ and $c \rightarrow u$ transitions. Bounds on $\Lambda/|\mathbb{C}_{ij}^{\text{DR}}|$ are identical.

D.2 Quark Vector Interactions

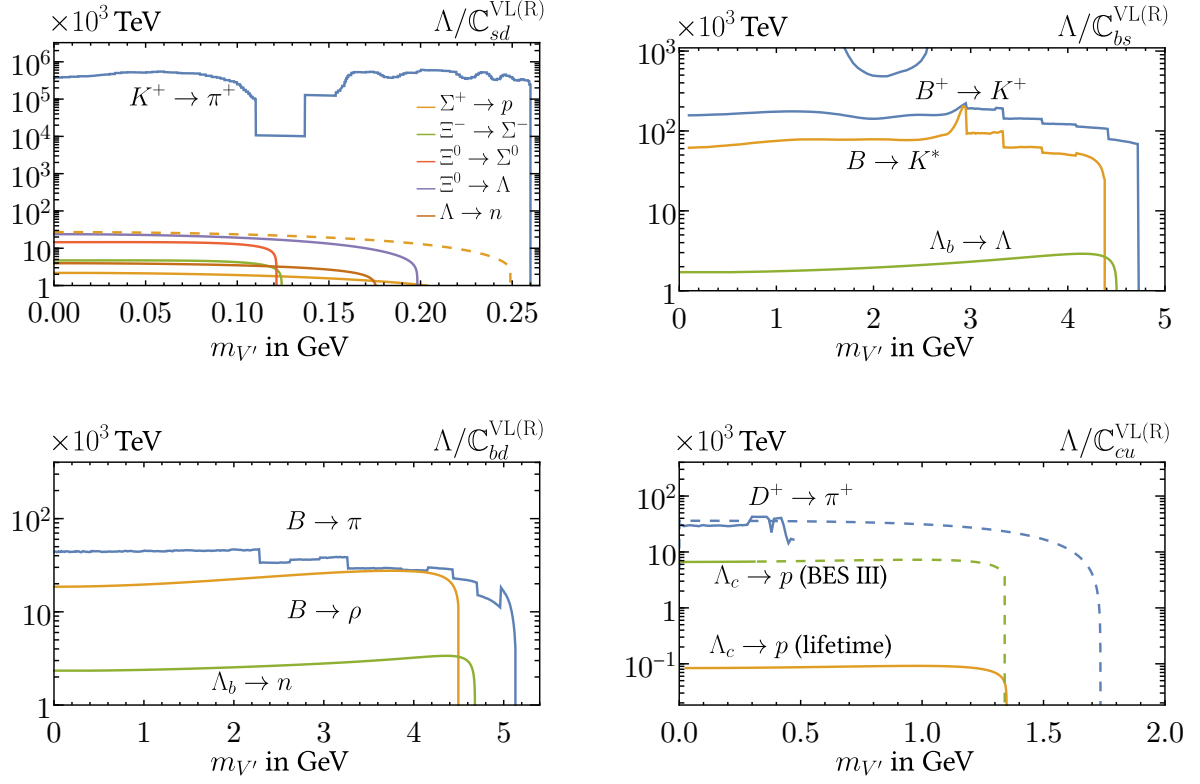


Figure 9: Upper limits on quark-flavor violating vector couplings $\Lambda/|C_{ij}^{VL}|$, for $s \rightarrow d$, $b \rightarrow s$, $b \rightarrow d$ and $c \rightarrow u$ transitions. Bounds on $\Lambda/|C_{ij}^{VR}|$ are identical.

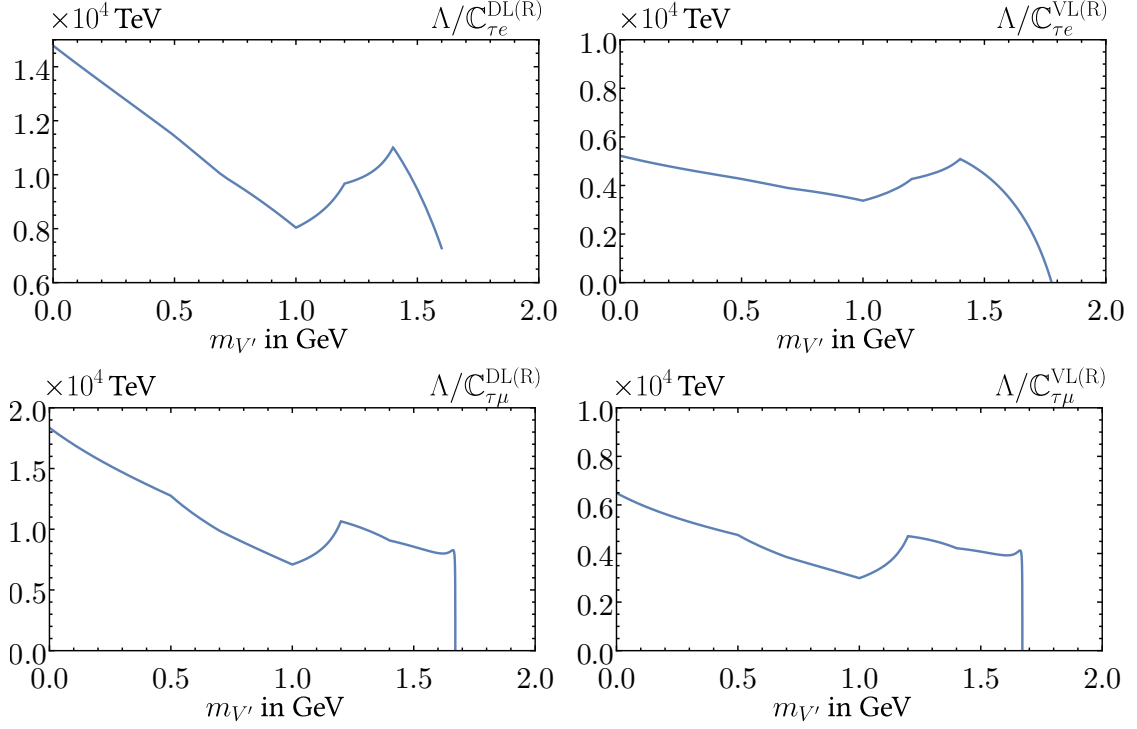


Figure 10: *Upper panel:* Lower limits on the dipole (left panel) and vector (right panel) couplings for $\tau \rightarrow e$ transitions $\Lambda/|\mathcal{C}_{\tau e}^{\text{DL(R)}}|$, $\Lambda/|\mathcal{C}_{\tau e}^{\text{VL(R)}}|$ from Belle II [38]. *Lower panel:* same for $\tau \rightarrow \mu$ transitions $\Lambda/|\mathcal{C}_{\tau \mu}^{\text{DL(R)}}|$, $\Lambda/|\mathcal{C}_{\tau \mu}^{\text{VL(R)}}|$.

E Two-body decays to Light Dark Vectors

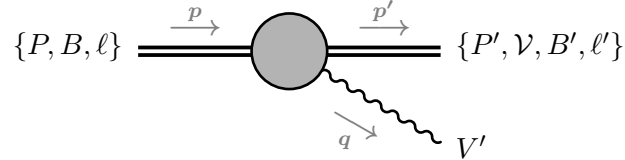


Figure 11: Two-body decays $\{P, B, \ell\} \rightarrow \{P', \mathcal{V}, B', \ell'\} + V'$. The blob represents the non-perturbative QCD effects for the hadronic decays.

In this appendix we present the full expressions for the two-body decays to a LDV that enter our analysis, namely

- $P \rightarrow P' + V'$: pseudoscalar meson to pseudoscalar meson and LDV,
- $P \rightarrow \mathcal{V} + V'$: pseudoscalar meson to vector meson and LDV,
- $B \rightarrow B' + V'$: baryon to baryon and LDV,
- $\ell \rightarrow \ell' + V'$: lepton to lepton and LDV.

For the hadronic processes illustrative Feynman diagrams are shown in Figure 1, while throughout this appendix we define the two-body kinematics for all decays as in Figure 11, namely as

$$\text{SM}(p) \rightarrow \text{SM}'(p') + V'(q) \quad (\text{E.1})$$

with $q = p - p'$ and $q^2 = (p - p')^2 = m_{V'}^2$. In the next subsection we collect the parametrization of all the relevant form factors for the hadronic processes considered, and in the subsequent subsections we present the expressions for the rates. The numerical values for the form-factors are always taken from the most recent work referenced.

E.1 Form Factors

$P \rightarrow P' + V'$

For these decays the hadronic matrix elements for the vector and axial-vector currents read [66]

$$\begin{aligned} \langle P'(p') | \bar{q}' \gamma^\mu q | P(p) \rangle &= (p + p')^\mu f_+^{PP'}(q^2) + (p - p')^\mu f_-^{PP'}(q^2), \\ \langle P'(p') | \bar{q}' \gamma_5 \gamma^\mu q | P(p) \rangle &= 0. \end{aligned} \quad (\text{E.2})$$

The corresponding matrix elements for tensor and pseudo-tensor currents read [66]

$$\begin{aligned} \langle P'(p') | \bar{q}' \sigma_{\mu\nu} q | P(p) \rangle &= \frac{2}{m_P + m_{P'}} (p'_\mu p_\nu - p'_\nu p_\mu) f_T^{PP'}(q^2), \\ \langle P'(p') | \bar{q}' \sigma^{\mu\nu} \gamma_5 q | P(p) \rangle &= \frac{2i}{m_P + m_{P'}} \epsilon^{\mu\nu\rho\sigma} p'_\rho p_\sigma f_{\bar{T}}^{PP'}(q^2), \end{aligned} \quad (\text{E.3})$$

where here and throughout we use the $\epsilon_{0123} = -\epsilon^{0123} = +1$ convention for the Levi-Civita tensor.

$P \rightarrow \mathcal{V} + V'$

For the pseudoscalar decays to two vectors with \mathcal{V} denoting the vector-meson, the hadronic matrix element for the vector and axial-vector currents are parametrized as [66]

$$\langle \mathcal{V}(p', \lambda) | \bar{q}' \gamma^\mu (1 \mp \gamma_5) q | P(p) \rangle = P_1^\mu \mathcal{V}_1(q^2) \pm P_2^\mu \mathcal{V}_2(q^2) \pm P_3^\mu \mathcal{V}_3(q^2) \pm P_P^\mu \mathcal{V}_P(q^2), \quad (\text{E.4})$$

where λ denotes the polarization of \mathcal{V} . The kinematic functions read

$$\begin{aligned} P_P^\mu &= i(\epsilon^* \cdot q) q^\mu, & P_1^\mu &= 2\epsilon^\mu_{\alpha\beta\gamma} \epsilon^{*\alpha} p'^\beta q^\gamma, \\ P_2^\mu &= i[(m_P^2 - m_{\mathcal{V}}^2) \epsilon^{*\mu} - (\epsilon^* \cdot q)(p' + p)^\mu], & P_3^\mu &= i(\epsilon^* \cdot q) \left[q^\mu - \frac{q^2}{m_P^2 - m_{\mathcal{V}}^2} (p' + p)^\mu \right], \end{aligned} \quad (\text{E.5})$$

where $\epsilon_\mu^* = \epsilon_\mu^*(p', \lambda)$ denotes the polarization vector of the outgoing \mathcal{V} . The scalar form factors can be further parametrized as

$$\begin{aligned} \mathcal{V}_P(q^2) &= \frac{-2m_{\mathcal{V}}}{q^2} A_0(m_{V'}^2), & \mathcal{V}_1(q^2) &= \frac{-V(q^2)}{m_P + m_{\mathcal{V}}}, & \mathcal{V}_2(q^2) &= \frac{-A_1(q^2)}{m_P - m_{\mathcal{V}}}, \\ \mathcal{V}_3(q^2) &= \frac{m_P + m_{\mathcal{V}}}{q^2} A_1(q^2) - \frac{m_P - m_{\mathcal{V}}}{q^2} A_2(q^2) \equiv \frac{2m_{\mathcal{V}}}{q^2} A_3(q^2), \end{aligned} \quad (\text{E.6})$$

with $A_3(0) = A_0(0)$, which ensures finite matrix elements at $q^2 = 0$, i.e., for massless LDV.

The corresponding matrix elements for tensor and pseudo-tensor currents read [66]

$$\begin{aligned}\langle \mathcal{V}(p', \lambda) | \bar{q}' \sigma^{\mu\nu} q | P(p) \rangle &= -i \epsilon_\alpha^* T^{\alpha\mu\nu}(q^2), \\ \langle \mathcal{V}(p', \lambda) | \bar{q}' \sigma_{\mu\nu} \gamma_5 q | P(p) \rangle &= \frac{1}{2} \epsilon_\alpha^* \epsilon_{\mu\nu\rho\sigma} T^{\alpha\rho\sigma}(q^2),\end{aligned}\tag{E.7}$$

where

$$\begin{aligned}T^{\alpha\mu\nu}(q^2) &= \epsilon^{\alpha\mu\nu\beta} \left[\left(p_\beta + p'_\beta - q_\beta \frac{m_P^2 - m_V^2}{q^2} \right) T_1^{PV}(q^2) + q_\beta \frac{m_P^2 - m_V^2}{q^2} T_2^{PV}(q^2) \right] \\ &+ \frac{2p^\alpha}{q^2} \epsilon^{\mu\nu\beta\gamma} p_\beta p'_\gamma \left(T_2^{PV}(q^2) - T_1^{PV}(q^2) + \frac{q^2}{m_P^2 - m_V^2} T_3^{PV}(q^2) \right).\end{aligned}\tag{E.8}$$

For vanishing momentum transfer $q^2 = 0$, i.e., massless LDV, the scalar form-factors satisfy

$$T_1^{PV}(0) = T_2^{PV}(0) \equiv T,\tag{E.9}$$

while the contribution proportional to $T_3(0)$ vanishes.

$B \rightarrow B' + V'$

For the baryon decays the matrix elements for vector and axial-vector currents are parametrized by [67, 69, 72]

$$\begin{aligned}\langle B'(p') | \bar{q}' \gamma_\mu q | B(p) \rangle &= \bar{u}_{B'}(p') \left(f_1(q^2) \gamma_\mu - i \frac{f_2(q^2)}{m_B} \sigma_{\mu\nu} q^\nu + \frac{f_3(q^2)}{m_B} q_\mu \right) u_B(p), \\ \langle B'(p') | \bar{q}' \gamma_\mu \gamma_5 q | B(p) \rangle &= \bar{u}_{B'}(p') \left(g_1(q^2) \gamma_\mu - i \frac{g_2(q^2)}{m_B} \sigma_{\mu\nu} q^\nu + \frac{g_3(q^2)}{m_B} q_\mu \right) \gamma_5 u_B(p),\end{aligned}\tag{E.10}$$

with $u_B(p)$ and $u_{B'}(p')$ the spinor functions for B and B' respectively. For Λ decays the values of the form factors are taken from [67, 69, 72], while for hyperon decays they are taken from [62–64].

The corresponding matrix elements for tensor and pseudo-tensor currents have the form [32, 79]

$$\begin{aligned}\langle B'(p') | \bar{q}' \sigma^{\mu\nu} q | B(p) \rangle &= g_T^{BB'} \bar{u}_{B'}(p') \sigma^{\mu\nu} u_B(p), \\ \langle B'(p') | \bar{q}' \sigma_{\mu\nu} \gamma_5 q | B(p) \rangle &= \frac{i}{2} g_T^{BB'} \epsilon_{\mu\nu\alpha\beta} \bar{u}_{B'}(p') \sigma^{\alpha\beta} u_B(p),\end{aligned}\tag{E.11}$$

which is an approximation valid for $m_{V'}^2 = 0$, which we use for the hyperon decays. For the baryon $\Lambda_b \rightarrow \Lambda$, $\Lambda_b \rightarrow n$, and $\Lambda_c \rightarrow p$ decays we use the available full parametrization, given by [67, 72]

$$\begin{aligned}\langle B'(p') | \bar{q}' i \sigma^{\mu\nu} q_\nu q | B(p) \rangle &= \bar{u}_{B'}(p') \left(\frac{f_1^{\text{TV}}(q^2)}{m_B} (\gamma^\mu q^2 - q^\mu \not{q}) - f_2^{\text{TV}}(q^2) i \sigma^{\mu\nu} q_\nu \right) u_B(p), \\ \langle B'(p') | \bar{q}' i \sigma^{\mu\nu} q_\nu \gamma_5 q | B(p) \rangle &= \bar{u}_{B'}(p') \left(\frac{f_1^{\text{TA}}(q^2)}{m_B} (\gamma^\mu q^2 - q^\mu \not{q}) - f_2^{\text{TA}}(q^2) i \sigma^{\mu\nu} q_\nu \right) \gamma_5 u_B(p).\end{aligned}$$

Having collected all hadronic input used in the analysis we next present the full expressions for the two-body rates. We show separately the contributions from dipole and vector interactions with the LDV, c.f. Eqs. (2.1) and (2.2). For brevity we drop the argument in all form factors since it is always $q^2 = m_{V'}^2$, in two-body decays. To shorten the expression we also introduce the notations

$$\kappa_x \equiv m_x^2/M^2 \quad \text{and} \quad \lambda_{xy} \equiv (1 - \kappa_x - \kappa_y)^2 - 4\kappa_x\kappa_y,$$

with m_x indicating the mass of the final-state particle x and M the mass of the decaying particle.

E.2 Partial width for $P \rightarrow P' + V'$

The partial width for the decay $P \rightarrow P' + V'$ with an underlying $q \rightarrow q'$ flavor-changing transition is given respectively for dipole and vector interaction by

$$\Gamma(P \rightarrow P'V')\Big|_{\text{D}} = \frac{\kappa_{V'} m_P^3}{4\pi\Lambda^2} \frac{\lambda_{P'V'}^{3/2}}{(1 + \sqrt{\kappa_{P'}})^2} |f_{\text{T}}^{PP'}|^2 |\mathbb{C}_{q'q}^{\text{D}}|^2, \quad (\text{E.12})$$

$$\Gamma(P \rightarrow P'V')\Big|_{\text{V}} = \frac{m_P^3}{16\pi\Lambda^2} \lambda_{P'V'}^{3/2} |f_{+}^{PP'}|^2 |\mathbb{C}_{q'q}^{\text{V}}|^2, \quad (\text{E.13})$$

Note that due to the parity conservation of strong interactions the rate is independent of the axial couplings $\mathbb{C}_{ij}^{\text{V}5}$ and $\mathbb{C}_{ij}^{\text{D}5}$. Therefore, $P \rightarrow P' + V'$ decays are only sensitive to the $\mathbb{C}_{ij}^{\text{V(D)}}$ couplings.

In the $\{\text{L}, \text{R}\}$ basis, these decays are sensitive to both $\mathbb{C}_{ij}^{\text{DL(R)}}$, $\mathbb{C}_{ij}^{\text{VL(R)}}$ couplings.

In the limit for massless LDV, the leading in $m_{V'}$ contributions to the decay rates read

$$\lim_{m_{V'} \rightarrow 0} \Gamma(P \rightarrow P' + V')\Big|_{\text{D}} = \frac{m_{V'}^2 m_P}{4\pi\Lambda^2} (1 - \sqrt{\kappa_{P'}})^3 |f_{\text{T}}^{PP'}|^2 |\mathbb{C}_{q'q}^{\text{D}}|^2, \quad (\text{E.14})$$

$$\lim_{m_{V'} \rightarrow 0} \Gamma(P \rightarrow P' + V')\Big|_{\text{V}} = \frac{m_P^3}{16\pi\Lambda^2} (1 - \kappa_{P'})^3 |f_{+}^{PP'}|^2 |\mathbb{C}_{q'q}^{\text{V}}|^2. \quad (\text{E.15})$$

While the rate originating from dipole interactions vanishes in the massless limit, the contribution of the vector interaction remains constant due to the linear scaling $m_{V'}/\Lambda$ introduced and discussed in Eq. (2.2).

E.3 Partial width for $P \rightarrow \mathcal{V} + V'$

The partial width for the decay $P \rightarrow \mathcal{V} + V'$ with an underlying $q \rightarrow q'$ flavor-changing transition is given respectively for dipole and vector interaction by

$$\Gamma(P \rightarrow \mathcal{V} + V')\Big|_{\text{D}} = \frac{m_P^3}{2\pi\Lambda^2} \lambda_{\mathcal{V}V'}^{1/2} (A_{\text{D}} |\mathbb{C}_{q'q}^{\text{D}}|^2 + A_{\text{D}5} |\mathbb{C}_{q'q}^{\text{D}5}|^2), \quad (\text{E.16})$$

$$\Gamma(P \rightarrow \mathcal{V} + V')\Big|_{\text{V}} = \frac{m_P^3 \kappa_{V'}^2}{8\pi\Lambda^2} \lambda_{\mathcal{V}V'}^{1/2} (A_{\text{V}} |\mathbb{C}_{q'q}^{\text{V}}|^2 + A_{\text{V}5} |\mathbb{C}_{q'q}^{\text{V}5}|^2),$$

with the coefficients A_X given by

$$A_{\text{D}} = |T_1^{P\mathcal{V}}|^2 \lambda_{\mathcal{V}V'}, \quad (\text{E.17})$$

$$A_{\text{D}5} = |T_2^{P\mathcal{V}}|^2 \frac{8\kappa_{\mathcal{V}}(1 - \kappa_{\mathcal{V}})^2 + \kappa_{V'}(1 + 3\kappa_{\mathcal{V}})^2 - 2\kappa_{V'}^2(1 + 3\kappa_{\mathcal{V}}) + \kappa_{V'}^3}{8\kappa_{\mathcal{V}}} \\ + |T_3^{P\mathcal{V}}|^2 \lambda_{\mathcal{V}V'}^2 \frac{\kappa_{V'}}{8\kappa_{\mathcal{V}}(1 - \kappa_{\mathcal{V}})^2} - \text{Re}(T_2^{P\mathcal{V}} T_3^{P\mathcal{V}*}) \lambda_{\mathcal{V}V'} \frac{\kappa_{V'}(1 + 3\kappa_{\mathcal{V}} - \kappa_{V'})}{4\kappa_{\mathcal{V}}(1 - \kappa_{\mathcal{V}})}, \quad (\text{E.18})$$

$$A_{\text{V}} = |V|^2 \frac{\lambda_{\mathcal{V}V'}}{(1 + \sqrt{\kappa_{\mathcal{V}}})^2}, \quad (\text{E.19})$$

$$A_{\text{V}5} = |A_1|^2 \frac{\kappa_{V'}^3 - 2\kappa_{V'}^2(1 + 3\kappa_{\mathcal{V}}) + \kappa_{V'}(1 + 3\kappa_{\mathcal{V}})^2 + 8(1 - \kappa_{\mathcal{V}})^2 \kappa_{\mathcal{V}}}{8\kappa_{\mathcal{V}}(1 - \sqrt{\kappa_{\mathcal{V}}})^2} \\ + |A_3|^2 \frac{\lambda_{\mathcal{V}V'}^2}{2\kappa_{V'}(1 - \kappa_{\mathcal{V}})^2} + \text{Re}(A_1 A_3^*) \frac{\sqrt{1 + \kappa_{\mathcal{V}}}}{2\sqrt{\kappa_{\mathcal{V}}}(1 - \kappa_{\mathcal{V}})^2} \lambda_{\mathcal{V}V'} (1 - \kappa_{V'} + 3\kappa_{\mathcal{V}}). \quad (\text{E.20})$$

In the limit of a massless LDV, the decay rates reduce to

$$\begin{aligned}\lim_{m_{V'} \rightarrow 0} \Gamma(P \rightarrow \mathcal{V}V') \Big|_{\text{D}} &= \frac{m_P^3}{2\pi\Lambda^2} (1 - \kappa_{\mathcal{V}})^3 |T|^2 (|\mathbb{C}_{q'q}^{\text{D}}|^2 + |\mathbb{C}_{q'q}^{\text{D}5}|^2), \\ \lim_{m_{V'} \rightarrow 0} \Gamma(P \rightarrow \mathcal{V}V') \Big|_{\text{V}} &= \frac{m_P^3}{16\pi\Lambda^2} (1 - \kappa_{\mathcal{V}})^3 \left(|A_3|^2 |\mathbb{C}_{q'q}^{\text{V}5}|^2 + \frac{2\kappa_{V'} |V|^2}{(\sqrt{\kappa_{\mathcal{V}}} + 1)^2} |\mathbb{C}_{q'q}^{\text{V}}|^2 \right),\end{aligned}\quad (\text{E.21})$$

which illustrates that the sensitivity to $\mathbb{C}_{q'q}^{\text{V}}$ weakens for very light LDVs.

E.4 Partial width for $B \rightarrow B' + V'$

For baryon decays $B \rightarrow B' + V'$ with an underlying $q \rightarrow q'$ transition the contribution to the partial width from the dipole and vector interaction read

$$\begin{aligned}\Gamma(B \rightarrow B'V') \Big|_{\text{D}} &= \frac{m_B^3}{4\pi\Lambda^2} \lambda_{B'V'}^{1/2} \left[(|f_1^{\text{TV}}|^2 \hat{A}_{\text{D}1}^- + |f_2^{\text{TV}}|^2 \hat{A}_{\text{D}2}^- + \hat{A}_{\text{D}12}^- \text{Re}(f_1^{\text{TV}} f_2^{\text{TV}*})) |\mathbb{C}_{q'q}^{\text{D}}|^2 \right. \\ &\quad \left. + (|f_1^{\text{TA}}|^2 \hat{A}_{\text{D}1}^+ + |f_2^{\text{TA}}|^2 \hat{A}_{\text{D}2}^+ + \hat{A}_{\text{D}12}^+ \text{Re}(f_1^{\text{TA}} f_2^{\text{TA}*})) |\mathbb{C}_{q'q}^{\text{D}5}|^2 \right], \\ \Gamma(B \rightarrow B'V') \Big|_{\text{V}} &= \frac{m_B^3}{16\pi\Lambda^2} \lambda_{B'V'}^{1/2} \left[(|f_1|^2 \hat{A}_{\text{V}1}^- + |f_2|^2 \hat{A}_{\text{V}2}^- + \hat{A}_{\text{V}12}^- \text{Re}(f_1 f_2^*)) |\mathbb{C}_{q'q}^{\text{V}}|^2 \right. \\ &\quad \left. + (|g_1|^2 \hat{A}_{\text{V}1}^+ + |g_2|^2 \hat{A}_{\text{V}2}^+ + \hat{A}_{\text{V}12}^+ \text{Re}(g_1 g_2^*)) |\mathbb{C}_{q'q}^{\text{V}5}|^2 \right],\end{aligned}\quad (\text{E.22})$$

with the kinematic coefficients

$$\begin{aligned}\hat{A}_{\text{D}1}^{\pm} &= \kappa_{V'} (\kappa_{B'}^2 + \kappa_{B'} (\kappa_{V'} - 2) \pm 6\sqrt{\kappa_{B'} \kappa_{V'}} - 2\kappa_{V'}^2 + \kappa_{V'} + 1), \\ \hat{A}_{\text{D}2}^{\pm} &= 2\kappa_{B'}^2 - \kappa_{B'} (\kappa_{V'} + 4) \pm 6\sqrt{\kappa_{B'} \kappa_{V'}} - \kappa_{V'}^2 - \kappa_{V'} + 2, \\ \hat{A}_{\text{D}12}^{\pm} &= 6\kappa_{V'} (\sqrt{\kappa_{B'}} \mp 1) (1 + \kappa_{B'} \pm 2\sqrt{\kappa_{B'}} - \kappa_{V'}), \\ \hat{A}_{\text{V}1}^{\pm} &= (1 + \kappa_{B'} \pm 2\sqrt{\kappa_{B'}} - \kappa_{V'}) (1 + \kappa_{B'} \mp 2\sqrt{\kappa_{B'}} + 2\kappa_{V'}), \\ \hat{A}_{\text{V}2}^{\pm} &= \kappa_{V'} (1 + \kappa_{B'} \pm 2\sqrt{\kappa_{B'}} - \kappa_{V'}) (2 + 2\kappa_{B'} \mp 4\sqrt{\kappa_{B'}} + \kappa_{V'}), \\ \hat{A}_{\text{V}12}^{\pm} &= 6\kappa_{V'} (\kappa_{B'} \pm 2\sqrt{\kappa_{B'}} - \kappa_{V'} + 1) (\sqrt{\kappa_{B'}} \mp 1).\end{aligned}$$

In the limit of a massless LDV, the rates reduce to

$$\begin{aligned}\lim_{m_{V'} \rightarrow 0} \Gamma(B \rightarrow B'V') \Big|_{\text{D}} &= \frac{m_B^3}{2\pi\Lambda^2} (1 - \kappa_{B'})^3 \left[|f_2^{\text{TV}}|^2 |\mathbb{C}_{q'q}^{\text{D}}|^2 + |f_2^{\text{TA}}|^2 |\mathbb{C}_{q'q}^{\text{D}5}|^2 \right], \\ \lim_{m_{V'} \rightarrow 0} \Gamma(B \rightarrow B'V') \Big|_{\text{V}} &= \frac{m_B^3}{16\pi\Lambda^2} (1 - \kappa_{B'})^3 \left(|f_1|^2 |\mathbb{C}_{q'q}^{\text{V}}|^2 + |g_1|^2 |\mathbb{C}_{q'q}^{\text{V}5}|^2 \right).\end{aligned}\quad (\text{E.23})$$

For hyperon decays we use the form factor parametrization of Eq. (E.11), valid for $m_{V'} = 0$. Nonetheless, we consider a massive LDV for the kinematics for completeness. The decay rate reads

$$\Gamma(B \rightarrow B'V') \Big|_{\text{D}} = \frac{m_B^3}{4\pi\Lambda^2} \lambda_{B'V'}^{1/2} (g_{\text{T}}^{BB'})^2 \left(\hat{A}_{\text{D}}^- |\mathbb{C}_{q'q}^{\text{D}}|^2 + \hat{A}_{\text{D}}^+ |\mathbb{C}_{q'q}^{\text{D}5}|^2 \right), \quad (\text{E.24})$$

with the kinematic coefficients

$$\hat{A}_{\text{D}}^{\pm} = (\kappa_{B'} \pm 2\sqrt{\kappa_{B'}} - \kappa_{V'} + 1) (2\kappa_{B'} \mp 4\sqrt{\kappa_{B'}} + \kappa_{V'} + 2). \quad (\text{E.25})$$

In the limit of a massless LDV, the rate reduces to

$$\lim_{m_{V'} \rightarrow 0} \Gamma(B \rightarrow B'V') \Big|_{\text{D}} = \frac{m_B^3}{2\pi\Lambda^2} (1 - \kappa_{B'})^3 |g_{\text{T}}^{BB'}|^2 \left(|\mathbb{C}_{q'q}^{\text{D}}|^2 + |\mathbb{C}_{q'q}^{\text{D}5}|^2 \right). \quad (\text{E.26})$$

For a fully polarized initial B , the differential width read

$$\begin{aligned} \frac{d\Gamma(B \rightarrow B'V')}{d \cos \theta} \Big|_{\text{D}} &= \frac{m_B^3}{8\pi\Lambda^2} \lambda_{B'V'}^{1/2} \left[\right. \\ &\quad \left(|f_1^{\text{TV}}|^2 \hat{A}_{\text{D}1}^- + |f_2^{\text{TV}}|^2 \hat{A}_{\text{D}2}^- + \hat{A}_{\text{D}12}^- \text{Re}(f_1^{\text{TV}} f_2^{\text{TV}*}) \right) |\mathbb{C}_{q'q}^{\text{D}}|^2 \\ &\quad + \left(|f_1^{\text{TA}}|^2 \hat{A}_{\text{D}1}^+ + |f_2^{\text{TA}}|^2 \hat{A}_{\text{D}2}^+ + \hat{A}_{\text{D}12}^+ \text{Re}(f_1^{\text{TA}} f_2^{\text{TA}*}) \right) |\mathbb{C}_{q'q}^{\text{D}5}|^2 \\ &\quad - 2\lambda_{B'V'}^{1/2} \cos \theta \left(\hat{B}_{\text{D}11} \text{Im}(f_1^{\text{TV}} f_1^{\text{TA}*}) + \hat{B}_{\text{D}12}^- \text{Im}(f_1^{\text{TV}} f_2^{\text{TA}*}) \right. \\ &\quad \quad \left. + \hat{B}_{\text{D}22} \text{Im}(f_2^{\text{TV}} f_2^{\text{TA}*}) + \hat{B}_{\text{D}12}^+ \text{Im}(f_2^{\text{TV}} f_1^{\text{TA}*}) \right) \text{Re}(\mathbb{C}_{q'q}^{\text{D}} \mathbb{C}_{q'q}^{\text{D}5*}) \\ &\quad - 2\lambda_{B'V'}^{1/2} \cos \theta \left(\hat{B}_{\text{D}11} \text{Re}(f_1^{\text{TV}} f_1^{\text{TA}*}) + \hat{B}_{\text{D}12}^- \text{Re}(f_1^{\text{TV}} f_2^{\text{TA}*}) \right. \\ &\quad \quad \left. + \hat{B}_{\text{D}22} \text{Re}(f_2^{\text{TV}} f_2^{\text{TA}*}) + \hat{B}_{\text{D}12}^+ \text{Re}(f_2^{\text{TV}} f_1^{\text{TA}*}) \right) \text{Im}(\mathbb{C}_{q'q}^{\text{D}} \mathbb{C}_{q'q}^{\text{D}5*}) \Big], \\ \frac{d\Gamma(B \rightarrow B'V')}{d \cos \theta} \Big|_{\text{V}} &= \frac{m_B^3}{32\pi\Lambda^2} \lambda_{B'V'}^{1/2} \left[\right. \\ &\quad \left(|f_1|^2 \hat{A}_{\text{V}1}^- + |f_2|^2 \hat{A}_{\text{V}2}^- + \hat{A}_{\text{V}12}^- \text{Re}(f_1 f_2^*) \right) |\mathbb{C}_{q'q}^{\text{V}}|^2 \\ &\quad + \left(|g_1|^2 \hat{A}_{\text{V}1}^+ + |g_2|^2 \hat{A}_{\text{V}2}^+ + \hat{A}_{\text{V}12}^+ \text{Re}(g_1 g_2^*) \right) |\mathbb{C}_{q'q}^{\text{V}5}|^2 \\ &\quad - 2\lambda_{B'V'}^{1/2} \cos \theta \left(\hat{B}_{\text{V}11} \text{Re}(f_1 g_1^*) + \hat{B}_{\text{V}12}^+ \text{Re}(f_2 g_1^*) \right. \\ &\quad \quad \left. + \hat{B}_{\text{V}12}^- \text{Re}(f_1 g_2^*) + \hat{B}_{\text{V}22} \text{Re}(f_2 g_2^*) \right) \text{Re}(\mathbb{C}_{q'q}^{\text{V}} \mathbb{C}_{q'q}^{\text{V}5*}) \\ &\quad + 2\lambda_{B'V'}^{1/2} \cos \theta \left(\hat{B}_{\text{V}11} \text{Im}(f_1 g_1^*) + \hat{B}_{\text{V}12}^+ \text{Im}(f_2 g_1^*) \right. \\ &\quad \quad \left. + \hat{B}_{\text{V}12}^- \text{Im}(f_1 g_2^*) + \hat{B}_{\text{V}22} \text{Im}(f_2 g_2^*) \right) \text{Im}(\mathbb{C}_{q'q}^{\text{V}} \mathbb{C}_{q'q}^{\text{V}5*}) \Big], \end{aligned} \quad (\text{E.27})$$

with the kinematic coefficients

$$\hat{B}_{\text{D}11} = \kappa_{V'} (\kappa_{B'} + 2\kappa_{V'} - 1), \quad \hat{B}_{\text{D}22} = 2\kappa_{B'} + \kappa_{V'} - 2, \quad \hat{B}_{\text{D}12}^{\pm} = -\kappa_{V'} (3\sqrt{\kappa_{B'}} \pm 1), \quad (\text{E.28})$$

$$\hat{B}_{\text{V}11} = \kappa_{B'} + 2\kappa_{V'} - 1, \quad \hat{B}_{\text{V}22} = \kappa_{V'} (2\kappa_{B'} + \kappa_{V'} - 2), \quad \hat{B}_{\text{V}12}^{\pm} = \kappa_{V'} (3\sqrt{\kappa_{B'}} \pm 1). \quad (\text{E.29})$$

In the limit of a massless LDV, the rate reduces to

$$\begin{aligned}
\lim_{m_{V'} \rightarrow 0} \frac{d\Gamma(B \rightarrow B'V')}{d \cos \theta} \Big|_{\text{D}} &= \frac{m_B^3}{4\pi\Lambda^2} (1 - \kappa_{B'})^3 \left[|f_2^{\text{TV}}|^2 |\mathbb{C}_{q'q}^{\text{D}}|^2 + |f_2^{\text{TA}}|^2 |\mathbb{C}_{q'q}^{\text{D}5}|^2 \right. \\
&\quad \left. + 2 \cos \theta (\text{Im}(f_2^{\text{TV}} f_2^{\text{TA}*}) \text{Re}(\mathbb{C}_{q'q}^{\text{D}} \mathbb{C}_{q'q}^{\text{D}5*}) + \text{Re}(f_2^{\text{TV}} f_2^{\text{TA}*}) \text{Im}(\mathbb{C}_{q'q}^{\text{D}} \mathbb{C}_{q'q}^{\text{D}5*})) \right], \\
\lim_{m_{V'} \rightarrow 0} \frac{d\Gamma(B \rightarrow B'V')}{d \cos \theta} \Big|_{\text{V}} &= \frac{m_B^3}{32\pi\Lambda^2} (1 - \kappa_{B'})^3 \left(|f_1|^2 |\mathbb{C}_{q'q}^{\text{V}}|^2 + |g_1|^2 |\mathbb{C}_{q'q}^{\text{V}5}|^2 \right. \\
&\quad \left. + 2 \cos \theta (\text{Re}(f_1 g_1^*) \text{Re}(\mathbb{C}_{q'q}^{\text{V}} \mathbb{C}_{q'q}^{\text{V}5*}) - \text{Im}(f_1 g_1^*) \text{Im}(\mathbb{C}_{q'q}^{\text{V}} \mathbb{C}_{q'q}^{\text{V}5*})) \right).
\end{aligned} \tag{E.30}$$

E.5 Polarized lepton distributions and rates $\ell \rightarrow \ell' + V'$

Next we consider the decays $\ell \rightarrow \ell' + V'$ for the case in which lepton-flavor violating dipole or vector interactions with the LDV are present. In this case there is experimental sensitivity to the polarization of the initial lepton by the measurement of the angular distribution of the angle θ , defined as the angle between the polarization vector of ℓ and the three-momentum of ℓ' . For the different LDV interactions we find for the differential width of a fully polarized initial ℓ

$$\begin{aligned}
\frac{d\Gamma(\ell \rightarrow \ell'V')}{d \cos \theta} \Big|_{\text{D}} &= \frac{m_\ell^3}{8\pi\Lambda^2} \lambda_{\ell'V'}^{1/2} \left[(\tilde{A}_+^{\text{D}} + \tilde{A}_-^{\text{D}}) |\mathbb{C}_{\ell'\ell}^{\text{D}}|^2 + (\tilde{A}_+^{\text{D}} - \tilde{A}_-^{\text{D}}) |\mathbb{C}_{\ell'\ell}^{\text{D}5}|^2 \right. \\
&\quad \left. + \tilde{A}_\theta^{\text{D}} \cos \theta \cdot \text{Im}(\mathbb{C}_{\ell'\ell}^{\text{D}} \mathbb{C}_{\ell'\ell}^{\text{D}5*}) \right], \\
\frac{d\Gamma(\ell \rightarrow \ell'V')}{d \cos \theta} \Big|_{\text{V}} &= \frac{m_\ell^3}{32\pi\Lambda^2} \lambda_{\ell'V'}^{1/2} \left[(\tilde{A}_+^{\text{V}} + \tilde{A}_-^{\text{V}}) |\mathbb{C}_{\ell'\ell}^{\text{V}}|^2 + (\tilde{A}_+^{\text{V}} - \tilde{A}_-^{\text{V}}) |\mathbb{C}_{\ell'\ell}^{\text{V}5}|^2 \right. \\
&\quad \left. + \tilde{A}_\theta^{\text{V}} \cos \theta \cdot \text{Re}(\mathbb{C}_{\ell'\ell}^{\text{V}} \mathbb{C}_{\ell'\ell}^{\text{V}5*}) \right],
\end{aligned} \tag{E.31}$$

with the kinematic coefficients

$$\begin{aligned}
\tilde{A}_+^{\text{D}} &= 2(1 - \kappa_{\ell'})^2 - \kappa_{V'}(1 + \kappa_{\ell'}) - \kappa_{V'}^2, & \tilde{A}_+^{\text{V}} &= (1 - \kappa_{\ell'})^2 + \kappa_{V'}(1 + \kappa_{\ell'}) - 2\kappa_{V'}^2, \\
\tilde{A}_-^{\text{D}} &= -6\sqrt{\kappa_{\ell'}\kappa_{V'}}, & \tilde{A}_-^{\text{V}} &= -6\sqrt{\kappa_{\ell'}\kappa_{V'}}, \\
\tilde{A}_\theta^{\text{D}} &= 2\lambda_{\ell'V'}^{1/2}(2 - 2\kappa_{\ell'} - \kappa_{V'}), & \tilde{A}_\theta^{\text{V}} &= 2\lambda_{\ell'V'}^{1/2}(1 - 2\kappa_{V'} - \kappa_{\ell'}).
\end{aligned} \tag{E.32}$$

In the limit of massless LDV, the polarized differential two-body rate reduces to

$$\begin{aligned}
\lim_{m_{V'} \rightarrow 0} \frac{d\Gamma(\ell \rightarrow \ell'V')}{d \cos \theta} \Big|_{\text{D}} &= \frac{m_\ell^3}{4\pi\Lambda^2} (1 - \kappa_{\ell'})^3 \left(|\mathbb{C}_{\ell'\ell}^{\text{D}}|^2 + |\mathbb{C}_{\ell'\ell}^{\text{D}5}|^2 + 2 \cos \theta \cdot \text{Im}(\mathbb{C}_{\ell'\ell}^{\text{D}} \mathbb{C}_{\ell'\ell}^{\text{D}5*}) \right) \\
\lim_{m_{V'} \rightarrow 0} \frac{d\Gamma(\ell \rightarrow \ell'V')}{d \cos \theta} \Big|_{\text{V}} &= \frac{m_\ell^3}{32\pi\Lambda^2} (1 - \kappa_{\ell'})^3 \left(|\mathbb{C}_{\ell'\ell}^{\text{V}}|^2 + |\mathbb{C}_{\ell'\ell}^{\text{V}5}|^2 + 2 \cos \theta \cdot \text{Re}(\mathbb{C}_{\ell'\ell}^{\text{V}} \mathbb{C}_{\ell'\ell}^{\text{V}5*}) \right).
\end{aligned} \tag{E.33}$$

Finally, after integrating over θ and averaging over the initial- and final-state polarizations, the total decay rates read

$$\Gamma(\ell \rightarrow \ell'V') \Big|_{\text{D}} = \frac{\lambda_{\ell'V'}^{1/2} m_\ell^3}{4\pi\Lambda^2} \left(|\mathbb{C}_{\ell'\ell}^{\text{D}}|^2 (\tilde{A}_+^{\text{D}} + \tilde{A}_-^{\text{D}}) + |\mathbb{C}_{\ell'\ell}^{\text{D}5}|^2 (\tilde{A}_+^{\text{D}} - \tilde{A}_-^{\text{D}}) \right), \tag{E.34}$$

$$\Gamma(\ell \rightarrow \ell' V') \Big|_{\text{V}} = \frac{\lambda_{\ell V'}^{1/2} m_\ell^3}{16\pi\Lambda^2} \left(|\mathbb{C}_{\ell'\ell}^{\text{V}}|^2 (\tilde{A}_+^{\text{V}} + \tilde{A}_-^{\text{V}}) + |\mathbb{C}_{\ell'\ell}^{\text{V}5}|^2 (\tilde{A}_+^{\text{V}} - \tilde{A}_-^{\text{V}}) \right), \quad (\text{E.35})$$

which in the limit of massless LDVs reduces to

$$\begin{aligned} \lim_{m_{V'} \rightarrow 0} \Gamma(\ell \rightarrow \ell' V') \Big|_{\text{D}} &= \frac{m_\ell^3}{2\pi\Lambda^2} (1 - \kappa_{\ell'})^3 \left(|\mathbb{C}_{\ell'\ell}^{\text{D}}|^2 + |\mathbb{C}_{\ell'\ell}^{\text{D}5}|^2 \right), \\ \lim_{m_{V'} \rightarrow 0} \Gamma(\ell \rightarrow \ell' V') \Big|_{\text{V}} &= \frac{m_\ell^3}{16\pi\Lambda^2} (1 - \kappa_{\ell'})^3 \left(|\mathbb{C}_{\ell'\ell}^{\text{V}}|^2 + |\mathbb{C}_{\ell'\ell}^{\text{V}5}|^2 \right). \end{aligned} \quad (\text{E.36})$$

References

- [1] S. Knapen, T. Lin and K.M. Zurek, *Light Dark Matter: Models and Constraints*, *Phys. Rev. D* **96** (2017) 115021 [[1709.07882](#)].
- [2] B. Holdom, *Two $U(1)$'s and Epsilon Charge Shifts*, *Phys. Lett. B* **166** (1986) 196.
- [3] B.A. Dobrescu, *Massless gauge bosons other than the photon*, *Phys. Rev. Lett.* **94** (2005) 151802 [[hep-ph/0411004](#)].
- [4] T. Hambye, M.H.G. Tytgat, J. Vandecasteele and L. Vanderheyden, *Dark matter from dark photons: a taxonomy of dark matter production*, *Phys. Rev. D* **100** (2019) 095018 [[1908.09864](#)].
- [5] E.J. Chun, J.-C. Park and S. Scopel, *Dark matter and a new gauge boson through kinetic mixing*, *JHEP* **02** (2011) 100 [[1011.3300](#)].
- [6] M. Fabbrichesi, E. Gabrielli and G. Lanfranchi, *The Dark Photon*, [2005.01515](#).
- [7] B.C. Allanach, J. Davighi and S. Melville, *An Anomaly-free Atlas: charting the space of flavour-dependent gauged $U(1)$ extensions of the Standard Model*, *JHEP* **02** (2019) 082 [[1812.04602](#)].
- [8] M. Williams, C.P. Burgess, A. Maharana and F. Quevedo, *New Constraints (and Motivations) for Abelian Gauge Bosons in the MeV-TeV Mass Range*, *JHEP* **08** (2011) 106 [[1103.4556](#)].
- [9] A. Smolkovič, M. Tamaro and J. Zupan, *Anomaly free Froggatt-Nielsen models of flavor*, *JHEP* **10** (2019) 188 [[1907.10063](#)].
- [10] Y. Kahn, G. Krnjaic, S. Mishra-Sharma and T.M.P. Tait, *Light Weakly Coupled Axial Forces: Models, Constraints, and Projections*, *JHEP* **05** (2017) 002 [[1609.09072](#)].
- [11] M. Bauer, P. Foldenauer and J. Jaeckel, *Hunting All the Hidden Photons*, *JHEP* **07** (2018) 094 [[1803.05466](#)].
- [12] A. Greljo, P. Stangl, A.E. Thomsen and J. Zupan, *On $(g - 2)_\mu$ from gauged $U(1)_X$* , *JHEP* **07** (2022) 098 [[2203.13731](#)].
- [13] R. Bause, H. Gisbert, G. Hiller, T. Höhne, D.F. Litim and T. Steudtner, *U -spin-CP anomaly in charm*, *Phys. Rev. D* **108** (2023) 035005 [[2210.16330](#)].
- [14] J. Brod, J. Drobnak, A.L. Kagan, E. Stamou and J. Zupan, *Stealth QCD-like strong interactions and the $t\bar{t}$ asymmetry*, *Phys. Rev. D* **91** (2015) 095009 [[1407.8188](#)].
- [15] A. Badin and A.A. Petrov, *Searching for light Dark Matter in heavy meson decays*, *Phys. Rev. D* **82** (2010) 034005 [[1005.1277](#)].
- [16] J.F. Kamenik and C. Smith, *FCNC portals to the dark sector*, *JHEP* **03** (2012) 090 [[1111.6402](#)].
- [17] E. Goudzovski et al., *New physics searches at kaon and hyperon factories*, *Rept. Prog. Phys.* **86** (2023) 016201 [[2201.07805](#)].
- [18] L. Calibbi, D. Redigolo, R. Ziegler and J. Zupan, *Looking forward to lepton-flavor-violating ALPs*, *JHEP* **09** (2021) 173 [[2006.04795](#)].

- [19] Y. Jho, S. Knapen and D. Redigolo, *Lepton-flavor violating axions at MEG II*, *JHEP* **10** (2022) 029 [2203.11222].
- [20] S. Knapen, K. Langhoff, T. Opferkuch and D. Redigolo, *A Robust Search for Lepton Flavour Violating Axions at Mu3e*, 2311.17915.
- [21] R.J. Hill, R. Plestid and J. Zupan, *Searching for new physics at $\mu \rightarrow e$ facilities with μ^+ and π^+ decays at rest*, 2310.00043.
- [22] J. Martin Camalich, M. Pospelov, P.N.H. Vuong, R. Ziegler and J. Zupan, *Quark Flavor Phenomenology of the QCD Axion*, *Phys. Rev. D* **102** (2020) 015023 [2002.04623].
- [23] J.L. Feng, T. Moroi, H. Murayama and E. Schnapka, *Third generation familons, B factories, and neutrino cosmology*, *Phys. Rev. D* **57** (1998) 5875 [hep-ph/9709411].
- [24] F. Björkeröth, E.J. Chun and S.F. King, *Flavourful Axion Phenomenology*, *JHEP* **08** (2018) 117 [1806.00660].
- [25] R. Ziegler, *Flavor Probes of Axion Dark Matter*, *PoS DISCRETE2022* (2024) 086 [2303.13353].
- [26] L.D. Landau, *On the angular momentum of a system of two photons*, *Dokl. Akad. Nauk SSSR* **60** (1948) 207.
- [27] C.-N. Yang, *Selection Rules for the Dematerialization of a Particle Into Two Photons*, *Phys. Rev.* **77** (1950) 242.
- [28] E. Gabrielli, B. Mele, M. Raidal and E. Venturini, *FCNC decays of standard model fermions into a dark photon*, *Phys. Rev. D* **94** (2016) 115013 [1607.05928].
- [29] M. Fabbrichesi, E. Gabrielli and B. Mele, *Hunting down massless dark photons in kaon physics*, *Phys. Rev. Lett.* **119** (2017) 031801 [1705.03470].
- [30] J.-Y. Su and J. Tandean, *Searching for dark photons in hyperon decays*, *Phys. Rev. D* **101** (2020) 035044 [1911.13301].
- [31] J.-Y. Su and J. Tandean, *Kaon decays shedding light on massless dark photons*, *Eur. Phys. J. C* **80** (2020) 824 [2006.05985].
- [32] J.M. Camalich, J. Terol-Calvo, L. Tolos and R. Ziegler, *Supernova Constraints on Dark Flavored Sectors*, *Phys. Rev. D* **103** (2021) L121301 [2012.11632].
- [33] NA62 collaboration, *Search for π^0 decays to invisible particles*, *JHEP* **02** (2021) 201 [2010.07644].
- [34] NA62 collaboration, *Measurement of the very rare $K^+ \rightarrow \pi^+ \nu \bar{\nu}$ decay*, *JHEP* **06** (2021) 093 [2103.15389].
- [35] BABAR collaboration, *A search for the decay $B^+ \rightarrow K^+ \nu \bar{\nu}$* , *Phys. Rev. Lett.* **94** (2005) 101801 [hep-ex/0411061].
- [36] BABAR collaboration, *Search for $B \rightarrow K^{(*)} \nu \bar{\nu}$ and invisible quarkonium decays*, *Phys. Rev. D* **87** (2013) 112005 [1303.7465].

- [37] CLEO collaboration, *Precision Measurement of $B(D^+ \rightarrow \mu^+ \nu)$ and the Pseudoscalar Decay Constant f_{D^+}* , *Phys. Rev. D* **78** (2008) 052003 [[0806.2112](#)].
- [38] BELLE-II collaboration, *Search for lepton-flavor-violating τ decays to a lepton and an invisible boson at Belle II*, [2212.03634](#).
- [39] BELLE-II collaboration, *Evidence for $B^+ \rightarrow K^+ \nu \bar{\nu}$ Decays*, [2311.14647](#).
- [40] BESIII collaboration, *Search for a massless dark photon in $\Lambda_c^+ \rightarrow p \gamma'$ decay*, *Phys. Rev. D* **106** (2022) 072008 [[2208.04496](#)].
- [41] TWIST collaboration, *Search for two body muon decay signals*, *Phys. Rev. D* **91** (2015) 052020 [[1409.0638](#)].
- [42] G. D'Ambrosio, G.F. Giudice, G. Isidori and A. Strumia, *Minimal flavor violation: An Effective field theory approach*, *Nucl. Phys. B* **645** (2002) 155 [[hep-ph/0207036](#)].
- [43] G. Isidori and D.M. Straub, *Minimal Flavour Violation and Beyond*, *Eur. Phys. J. C* **72** (2012) 2103 [[1202.0464](#)].
- [44] H. Ruegg and M. Ruiz-Altaba, *The Stueckelberg field*, *Int. J. Mod. Phys. A* **19** (2004) 3265 [[hep-th/0304245](#)].
- [45] B. Kors and P. Nath, *A Stueckelberg extension of the standard model*, *Phys. Lett. B* **586** (2004) 366 [[hep-ph/0402047](#)].
- [46] B. Kors and P. Nath, *Aspects of the Stueckelberg extension*, *JHEP* **07** (2005) 069 [[hep-ph/0503208](#)].
- [47] A. DiFranzo, P.J. Fox and T.M.P. Tait, *Vector Dark Matter through a Radiative Higgs Portal*, *JHEP* **04** (2016) 135 [[1512.06853](#)].
- [48] M. Zaazoua, L. Truong, K.A. Assamagan and F. Fassi, *Higgs Portal Vector Dark Matter Interpretation: Review of Effective Field Theory Approach and Ultraviolet Complete Models*, *LHEP* **2022** (2022) 270 [[2107.01252](#)].
- [49] S. Baek, P. Ko and W.-I. Park, *Addendum to "Invisible Higgs decay width versus dark matter direct detection cross section in Higgs portal dark matter models"*, *Phys. Rev. D* **105** (2022) 015007 [[2112.11983](#)].
- [50] G. Arcadi, J.C. Criado and A. Djouadi, *Iteration on the Higgs-portal for vector Dark Matter and its effective field theory description*, [2312.14052](#).
- [51] C.D. Froggatt and H.B. Nielsen, *Hierarchy of Quark Masses, Cabibbo Angles and CP Violation*, *Nucl. Phys. B* **147** (1979) 277.
- [52] D. Barducci, M. Nardecchia and C. Toni, *Perturbative unitarity constraints on generic vector interactions*, [2306.11533](#).
- [53] J. Folch Eguren, E. Stamou, M. Tabet and R. Ziegler, *to appear*, .
- [54] J. Albrecht, E. Stamou, R. Ziegler and R. Zwicky, *Flavoured axions in the tail of $B_q \rightarrow \mu^+ \mu^-$ and $B \rightarrow \gamma^*$ form factors*, *JHEP* **21** (2020) 139 [[1911.05018](#)].

- [55] ALEPH collaboration, *Measurements of BR ($b \rightarrow \tau \bar{\nu}_\tau X$) and BR ($b \rightarrow \tau^- \bar{\nu}_\tau D^{*\pm} X$) and upper limits on BR ($B^- \rightarrow \tau^- \bar{\nu}_\tau$) and BR ($b \rightarrow s \nu \bar{\nu}$)*, *Eur. Phys. J. C* **19** (2001) 213 [[hep-ex/0010022](#)].
- [56] G. Alonso-Álvarez and M. Escudero, *The first limit on invisible decays of B_s mesons comes from LEP*, [2310.13043](#).
- [57] W. Altmannshofer, A. Crivellin, H. Haigh, G. Inguglia and J. Martin Camalich, *Light New Physics in $B \rightarrow K^{(*)} \nu \bar{\nu}$?*, [2311.14629](#).
- [58] PARTICLE DATA GROUP collaboration, *Review of Particle Physics*, *PTEP* **2022** (2022) 083C01.
- [59] BESIII collaboration, *Search for the decay $D^0 \rightarrow \pi^0 \nu \bar{\nu}$* , *Phys. Rev. D* **105** (2022) L071102 [[2112.14236](#)].
- [60] I. Baum, V. Lubicz, G. Martinelli, L. Orifici and S. Simula, *Matrix elements of the electromagnetic operator between kaon and pion states*, *Phys. Rev. D* **84** (2011) 074503 [[1108.1021](#)].
- [61] ETM collaboration, *$K \rightarrow \pi l \nu$ Semileptonic Form Factors from Two-Flavor Lattice QCD*, *Phys. Rev. D* **80** (2009) 111502 [[0906.4728](#)].
- [62] T. Ledwig, J. Martin Camalich, L.S. Geng and M.J. Vicente Vacas, *Octet-baryon axial-vector charges and $SU(3)$ -breaking effects in the semileptonic hyperon decays*, *Phys. Rev. D* **90** (2014) 054502 [[1405.5456](#)].
- [63] N. Cabibbo, E.C. Swallow and R. Winston, *Semileptonic hyperon decays*, *Ann. Rev. Nucl. Part. Sci.* **53** (2003) 39 [[hep-ph/0307298](#)].
- [64] J.M. Gaillard and G. Sauvage, *HYPERON BETA DECAYS*, *Ann. Rev. Nucl. Part. Sci.* **34** (1984) 351.
- [65] BESIII collaboration, *Search for a massless particle beyond the Standard Model in the $\Sigma^+ \rightarrow p +$ invisible decay*, [2312.17063](#).
- [66] N. Gubernari, A. Kokulu and D. van Dyk, *$B \rightarrow P$ and $B \rightarrow V$ Form Factors from B -Meson Light-Cone Sum Rules beyond Leading Twist*, *JHEP* **01** (2019) 150 [[1811.00983](#)].
- [67] W. Detmold and S. Meinel, *$\Lambda_b \rightarrow \Lambda \ell^+ \ell^-$ form factors, differential branching fraction, and angular observables from lattice QCD with relativistic b quarks*, *Phys. Rev. D* **93** (2016) 074501 [[1602.01399](#)].
- [68] D. Leljak, B. Melić and D. van Dyk, *The $\bar{B} \rightarrow \pi$ form factors from QCD and their impact on $|V_{ub}|$* , *JHEP* **07** (2021) 036 [[2102.07233](#)].
- [69] W. Detmold, C. Lehner and S. Meinel, *$\Lambda_b \rightarrow p \ell^- \bar{\nu}_\ell$ and $\Lambda_b \rightarrow \Lambda_c \ell^- \bar{\nu}_\ell$ form factors from lattice QCD with relativistic heavy quarks*, *Phys. Rev. D* **92** (2015) 034503 [[1503.01421](#)].
- [70] ETM collaboration, *Tensor form factor of $D \rightarrow \pi(K) l \nu$ and $D \rightarrow \pi(K) l l$ decays with $N_f = 2 + 1 + 1$ twisted-mass fermions*, *Phys. Rev. D* **98** (2018) 014516 [[1803.04807](#)].
- [71] ETM collaboration, *Scalar and vector form factors of $D \rightarrow \pi(K) l \nu$ decays with $N_f = 2 + 1 + 1$ twisted fermions*, *Phys. Rev. D* **96** (2017) 054514 [[1706.03017](#)].
- [72] S. Meinel, *$\Lambda_c \rightarrow N$ form factors from lattice QCD and phenomenology of $\Lambda_c \rightarrow n \ell^+ \nu_\ell$ and $\Lambda_c \rightarrow p \mu^+ \mu^-$ decays*, *Phys. Rev. D* **97** (2018) 034511 [[1712.05783](#)].

- [73] A. Jodidio et al., *Search for Right-Handed Currents in Muon Decay*, *Phys. Rev. D* **34** (1986) 1967.
- [74] J.A. Dror, R. Lasenby and M. Pospelov, *Dark forces coupled to nonconserved currents*, *Phys. Rev. D* **96** (2017) 075036 [[1707.01503](#)].
- [75] M. Leurer, Y. Nir and N. Seiberg, *Mass matrix models*, *Nucl. Phys. B* **398** (1993) 319 [[hep-ph/9212278](#)].
- [76] L. Calibbi, Z. Lalak, S. Pokorski and R. Ziegler, *The Messenger Sector of SUSY Flavour Models and Radiative Breaking of Flavour Universality*, *JHEP* **06** (2012) 018 [[1203.1489](#)].
- [77] E.E. Jenkins, A.V. Manohar and M. Trott, *Renormalization Group Evolution of the Standard Model Dimension Six Operators II: Yukawa Dependence*, *JHEP* **01** (2014) 035 [[1310.4838](#)].
- [78] J. Aebischer and J. Kumar, *Flavour violating effects of Yukawa running in SMEFT*, *JHEP* **09** (2020) 187 [[2005.12283](#)].
- [79] R. Gupta, B. Yoon, T. Bhattacharya, V. Cirigliano, Y.-C. Jang and H.-W. Lin, *Flavor diagonal tensor charges of the nucleon from (2+1+1)-flavor lattice QCD*, *Phys. Rev. D* **98** (2018) 091501 [[1808.07597](#)].